國立交通大學

資訊科學與工程研究所

碩 士 論 文

利用紋理合成及形態學運算做彩色影像修補之研究

Color Image Inpainting using Texture Synthesis and Morphological Operations

研 究 生：呂盈賢

指導教授：薛元澤　教授

中 華 民 國 九 十 五 年 六 月

利 用 紋 理 合 成 及 形 態 學 運 算 做 彩 色 影 像 修 補 之 研 究

Color Image Inpainting using Texture Synthesis and Morphological Operations

研 究 生：呂盈賢　　　　Student：Ying-Shian Lu

指導教授：薛元澤　　　　Advisor：Yuang-Cheh Hsueh

國 立 交 通 大 學
資 訊 科 學 與 工 程 研 究 所
碩 士 論 文

A Thesis

Submitted to Institute of Computer Science and Engineering

College of Computer Science

National Chiao Tung University

in partial Fulfillment of the Requirements

for the Degree of

Master

in

Computer Science

June 2006

Hsinchu, Taiwan, Republic of China

中華民國九十五年六月

利用紋理合成及形態學運算做彩色影像修補之研究

學生：呂盈賢　　　　　　　　　　　　　　　　　指導教授：薛元澤

國 立 交 通 大 學
資 訊 科 學 與 工 程 研 究 所

摘要

為了修補影像中受損的區域，或是移除影像中的某個物件，常常必須使用影像修補的技術。因此如何有效且正確的修補一塊未知的區域便成為一個重要的研究領域。本論文嘗試使用紋理合成及形態學運算來做影像修補。實作上先使用數學形態學的 Opening 將受損區域分為兩大部分，其中一部分是影像中受損極小的區域，另一部分則是受損範圍較大的區域。針對受損極小的區域，計算周圍可用灰階值的平均值進行修補。而針對受損範圍較大的區域，則尋找影像中最相近的紋理來修補，同時，應用 FFT 區塊比對法去加速搜尋的時間。實驗結果顯示我們所提出的方法不僅能獲得令人滿意的修補品質，且在運算的時間上是相當有效率的。

Color Image Inpainting using Texture Synthesis and Morphological Operations

student：Ying-Shian Lu Advisors：Dr.Yuang-Cheh Hsueh

Institute of Computer Science and Engineering
College of Computer Science
National Chiao Tung University

ABSTRACT

Inpainting, techniques can repair damaged photographs and remove/replace selected objects on the image. The goals and applications of inpainting are numerous. How to effectively and correctly inpaint an unknown region has become an important research topic. In this thesis, we propose a new inpainting method by using texture synthesis and morphological operations. Based on mathematical morphology, we first use opening to split damaged regions into two parts. One consists of small damaged regions and the other consists of large damaged regions on the image. We inpaint the pixel in the small damaged regions by computing the average of undamaged neighboring pixels surrounding it. For the large damaged regions, we search the most similar texture to synthesize it. Simultaneously, we apply the FFT block matching algorithm to speedup the time of searching similar textures. The proposed method is computational efficient. Experimental results look "reasonable" to the human eye.

誌謝

我在這裡要感謝我的指導教授 薛元澤教授，兩年來對我孜孜不倦的教誨，教導我研究學問的方法及待人處世道理，讓我畢生受益無窮，以及我的口試委員 張隆紋教授 與 莊仁輝教授，二位老師不吝指教，讓這篇論文更加完善。

我還要感謝莊逢軒學長、何昌憲學長，給予我論文研究及寫作方面等的各種建議，感謝江仲庭同學、劉裕泉同學、王慧縈同學、顏佩君同學、林明志同學在這兩年內與我共同努力，互相砥礪，陪我度過這段快樂的實驗室生活。

僅將此論文獻給我親愛的家人與朋友，我的父母及弟弟，感謝他們在這段期間給我的關心、支持與鼓勵，祝福他們永遠健康快樂。

呂盈賢

謹誌於 國立交通大學資訊科學與工程研究所

中華民國九十五年六月

CONTENTS

LIST OF FIGURES

LIST OF TABLES

CHAPTER 1

Introduction

1.1 Motivation

The modification of images in a way that is non-detectable for an observer who does not know the original image is a practice as old as artistic creation itself. Medieval artwork started to be restored as early as the Renaissance. This practice is called retouching or inpainting. Traditionally, skilled artists have performed image inpainting manually. With the rapid development of digital life, the automatic inpainting techniques are developed.

The applications of image inpainting include the restoration of photographs (Fig. 1-1), films and paintings, the removal of objects (Fig. 1-2 to 1-3) and occlusions, such as text, subtitles (Fig. 1-4), stamps and publicity from images, image coding [5] (The objective is to retain only the information which cannot be correctly reconstructed "minute but important details" and to remove as much as possible from the remainder of the image. After data has been transmitted, using inpainting method to reconstruct the image. Fig. 1-5 shows an example. It reduces about 25% data transmission). In addition, inpainting can also be used to produce special effects (Fig. 1-6) and attack against visible watermarking [17].

Because the applications of image inpainting are living, how to effectively and correctly inpaint an unknown region has become an important research issue. In other words, image inpainting has become a paramount research topic in recent year. We are interested in knowing the well-known inpainting methods. The basic idea is to use undamaged neighboring information to inpaint damaged regions. In section 1.2, we will introduce several well-known inpainting methods and then direct several defects of them. In section 1.3, we will propose a new method that can improve these defects and get better performance.

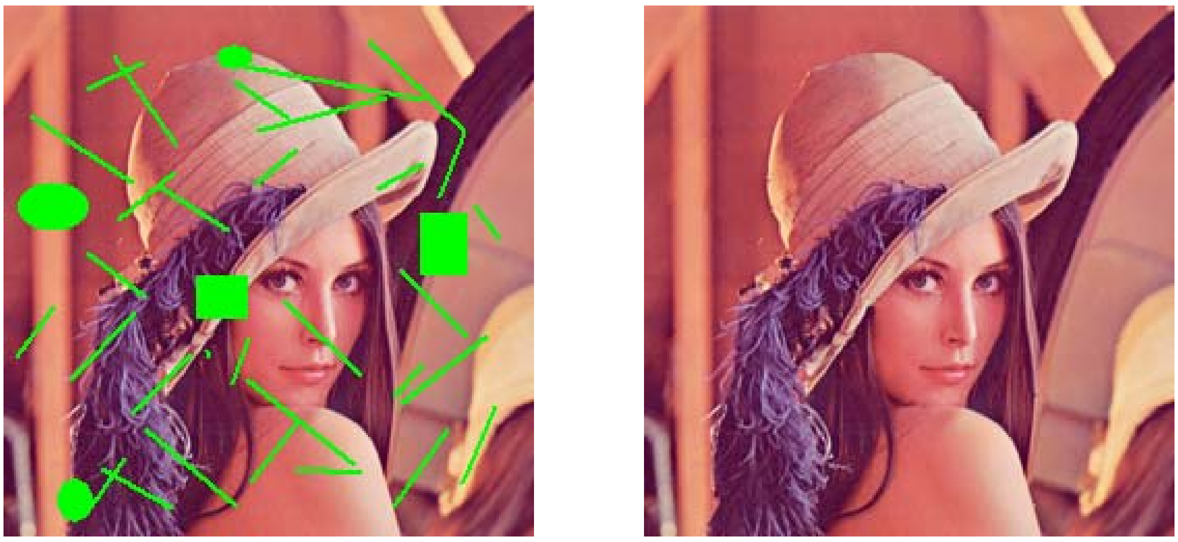

Fig. 1- 1 Restoration of photographs

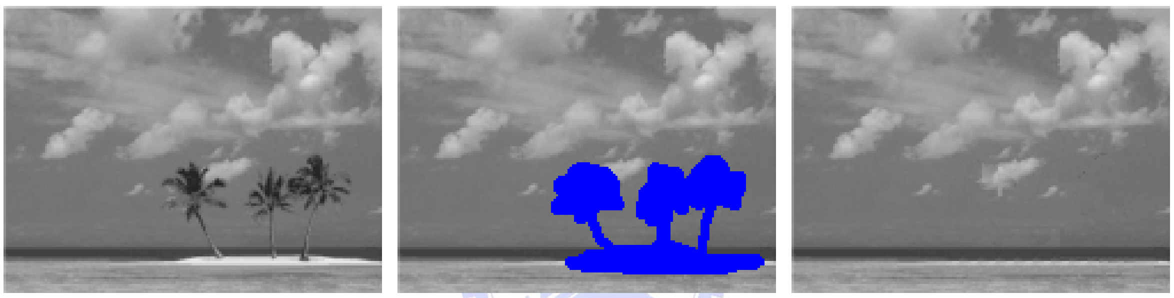

Fig. 1- 2 Removal of trees

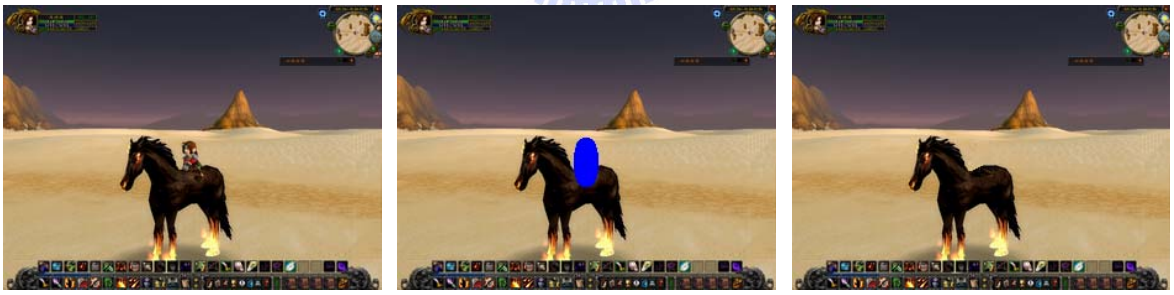

Fig. 1- 3 Removal of a girl

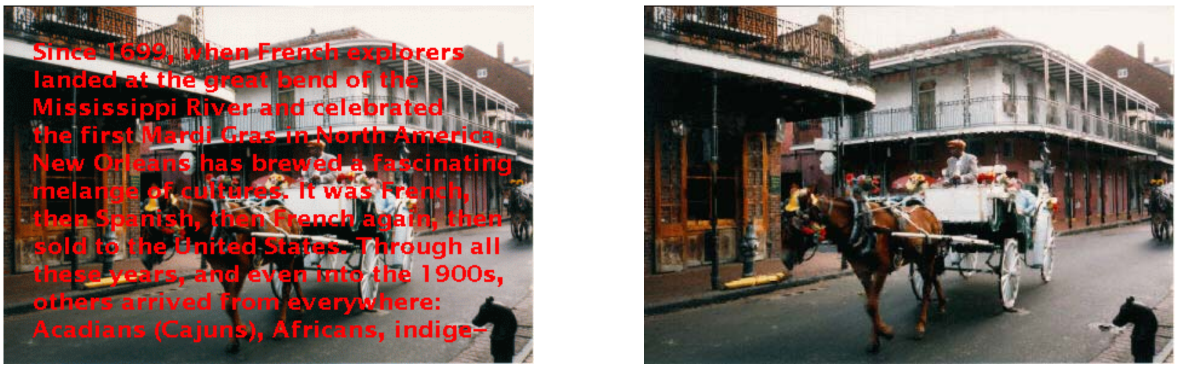

Since 1699, when French explorers landed at the great bend of the Mississippi River and celebrated the first Mardi Gras in North America, New Orleans has brewed a fascinating melange of cultures. It was French, then Spanish, then French again, then sold to the United States. Through all these years, and even into the 1900s, others arrived from everywhere: Acadians (Cajuns), Africans, indige-

Fig. 1- 4 Removal of subtitles

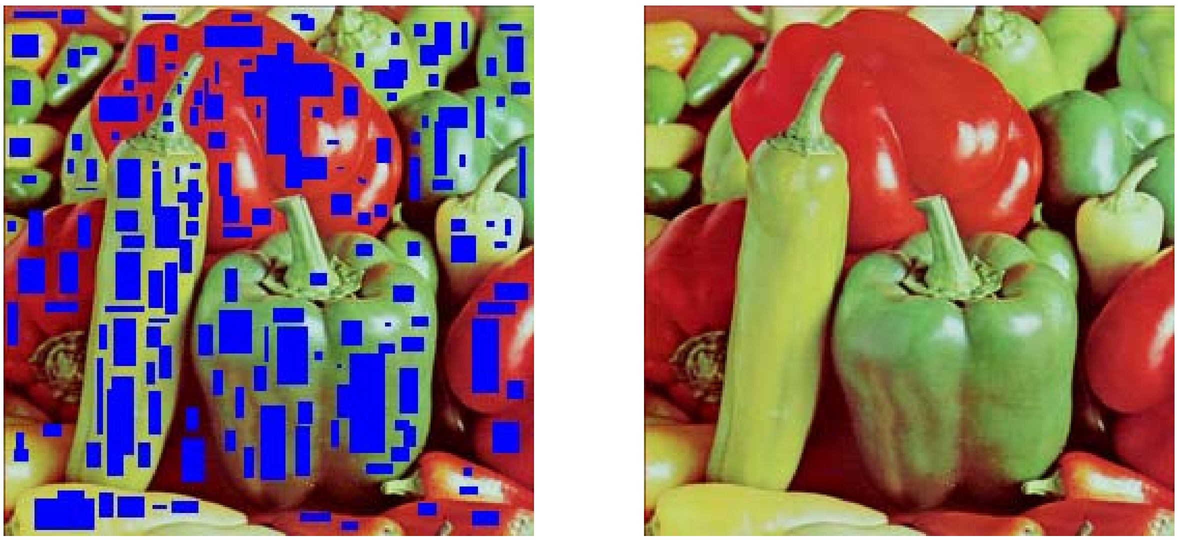

Fig. 1- 5 Applications of image coding

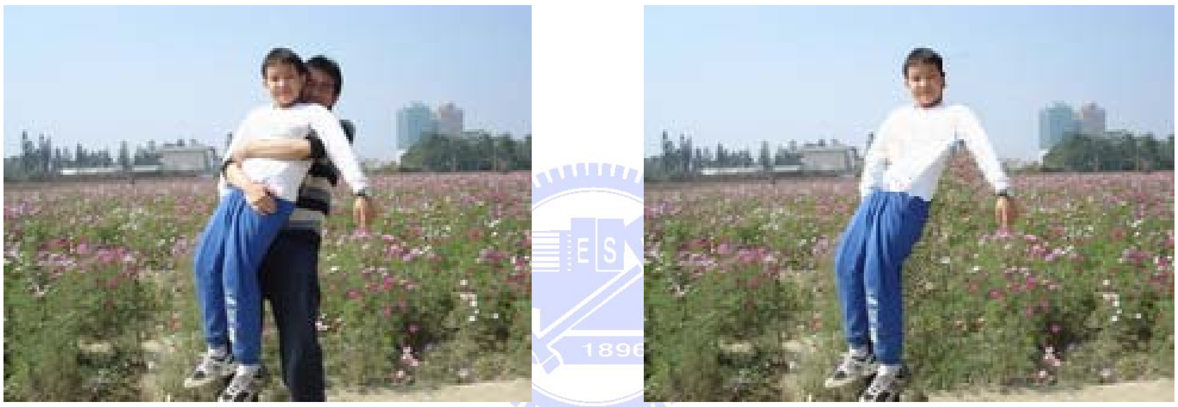

Fig. 1- 6 Special effects

1.2 Related Works

There are several researches of image inpainting. Bertalmio et al [1] have introduced a technique for digital inpainting of still images that produces very impressive results. Based on partial differential equations (PDEs), the algorithm fills in the damaged areas to be inpainted by propagating information from the outside of the masked region along level lines (Isophotes).

However, the algorithm usually requires several minutes on current personal computers for the inpainting of relatively small areas. Such a time is unacceptable for interactive sessions and motivated Manuel M. Oliveira, Brian Bowen, Richard McKenna and Yu-Sung Chang [2] to design a simpler and faster algorithm capable of producing similar results in just a few seconds. It uses a weighted average kernel that only considers contributions from the neighboring pixels. Efficiency of the fast inpainting algorithm is two to three orders of magnitude faster than those using partial differential equations. But it constraints the regions to be inpainted must be locally small. If the damaged regions are not small enough, some possibly important information might be discarded. Results might be blurred.

For inpainting large damaged regions well, Efros and Leung et al. [3] proposed a texture synthesis algorithm to solve the problem. In their algorithm, the lost region is filled-in pixel by pixel with the texture from its neighbors. This algorithm is considerably faster when using the improvements in [10], [18], [19], [20].

Inspired by the work of Efros and Leung [3], Criminisi, Pérez and Toyama proposed an exemplar-based texture synthesis algorithm [7] for removing/inpainting large objects from digital images. Their approach employs an exemplar-based texture synthesis technique modulated by a unified scheme for determining the fill order of the target region. Pixels maintain a confidence value, which together with image isophotes, influence their fill priority.

Viewing from above inpainting techniques, “Fast Digital Image Inpainting” [2] can fast inpaint small damaged regions, but it can’t work well for large damaged regions. “Region Filling and Object Removal by Exemplar-Based Image Inpainting” is also called “Priority Texture Synthesis” [7]. It can both inpaint small and large damaged regions well, but it spend too much time. Therefore, how to correctly and quickly inpaint these images with several small and large damaged regions becomes the goal of our paper.

1.3 Thesis Organization

In this thesis, we propose an image inpainting method that will combine “Fast Digital Image Inpainting” and “Priority Texture Synthesis”. The remainder of this thesis is organized as follows. In chapter 2, we will survey the research of image inpainting and discuss some issues needed to concern. Then, we will describe how to evaluate the similarity value between two textures. Finally, we will survey the concept of morphological operations. In chapter 3, we will present our method which uses the morphological operator “opening” to split the damaged regions of images into several small and large parts according to the structuring element which users set up. After splitting, we modify the “Fast Digital Image Inpainting” algorithm and apply it to inpaint small damaged parts. Then, we use “Priority Texture Synthesis” to inpaint large damaged parts and add the FFT block matching algorithm to speedup the time of searching similar textures. In chapter 4, we will experiment with different kinds of damaged images. The proposed method can efficiently reduce the cost of computation. Experimental results look “reasonable” to the human eye. Then, we will compare the performance of our method with other methods. In chapter 5, the conclusion and future work will be stated.

CHAPTER 2

Previous Research

In this chapter, we will describe several related researches about image inpainting in section 2.1. In section 2.2, we will describe the block matching problem and introduce a faster algorithm for solving it. In section 2.3, the concept of PSNR will be introduced. Basic morphological operators will be described in section 2.4.

2.1 Review of Digital Image Inpainting

The image inpainting methods are widely used in various fields such as wireless communication, reverting deterioration of photographs, image coding (e.g., recovering lost blocks) and special effects (e.g., removal of objects), etc. The basic idea behind the methods that have been proposed in the literature is to fill-in these regions with available information from their surroundings. In this section, we will describe some existed image inpainting algorithms.

2.1.1 Image Inpainting Based on Partial Differential Equation (PDE)

Bertalmio et al [1] pioneered a digital image-inpainting algorithm based on partial differential equations (PDEs). For the damaged image, it fills in the areas to be inpainted by propagating information from the outside of the masked region along level lines (Isophotes). Isophote directions are obtained by computing at each pixel along the inpainting contour a discretized gradient vector (it gives the direction of largest spatial change) and by rotating the resulting vector by 90 degrees (Fig. 2-1 [1]). This intends to propagate information while preserving edges. A 2-D Laplacian [21] is used to locally estimate the variation in color smoothness and such variation is propagated along the isophote direction [1]. After every few step of the inpainting process, the algorithm runs a few diffusion iterations to smooth the inpainted region.

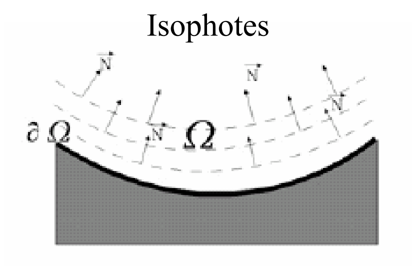

Fig. 2- 1 The figure describes what is Isophote Directions . Propagation direction as the normal to the signed distance to the boundary of the region to be inpainted.

The algorithm of that form can be written as :

$$I^{n+1}(i,j) = I^{n}(i,j) + \Delta t I_t^{n}(i,j), \quad \forall (i,j) \in \Omega \tag{2.1}$$

where the superindex *n* denotes the inpainting "time", (*i, j*) are the pixel coordinates, Δt is the rate of improvement and $I_t^n(i,j)$ stands for the update of the image $I^n(i,j)$. Note that the evolution equation runs only inside Ω, the region to be inpainted.

With this equation, the image $I^{n+1}(i,j)$ is an improved version of $I^n(i,j)$, with the "improvement" given by $I_t^n(i,j)$. As *n* increases, we achieve a better image. In section 2.1.1.1, we will introduce how to design the update $I_t^n(i,j)$.

2.1.1.1 How to calculate $I_t^n(i,j)$?

$I_t^n(i,j)$ stands for the update of the image $I^n(i,j)$. We use partial differential equations to compute it. It can be denoted as :

$$I_t^n(i,j) = \overrightarrow{\delta L^n}(i,j) \cdot \overrightarrow{N^n}(i,j) \tag{2.2}$$

where $\overrightarrow{\delta L}^n(i,j)$ is a measure of the change in the information $L^n(i,j)$. With this equation, we estimate the information $L^n(i,j)$ of our image and compute its change along the $\overrightarrow{N}$ direction. Note that at steady state, that is, when the equation (2.1) converges, $I^{n+1}(i,j) = I^n(i,j)$ and from (2.1) and (2.2) we have that $\overrightarrow{\delta L}^n(i,j) \cdot \overrightarrow{N}^n(i,j) = 0$, meaning exactly that the information L has been propagated in the direction $\overrightarrow{N}$. For more details, we now rewrite the equation (2.2) as :

$$I_t^n(i,j) = \left(\overrightarrow{\delta L}^n(i,j) \cdot \frac{\overrightarrow{N}(i,j,n)}{\left|\overrightarrow{N}(i,j,n)\right|} \right) \left|\nabla I^n(i,j)\right| \tag{2.3}$$

On the implementation, we can use discrete equation borrows from the numerical analysis literature. See Section 2.1.1.2, Section 2.1.1.3 and Section 2.1.1.4.

2.1.1.2 How to calculate $\overrightarrow{\delta L}^n(i,j)$?

$$\overrightarrow{\delta L}^n(i,j) := \left(L^n(i+1,j) - L^n(i-1,j), L^n(i,j+1) - L^n(i,j-1)\right) \tag{2.4}$$

$$L^n(i,j) = I_{xx}^n(i,j) + I_{yy}^n(i,j) \tag{2.5}$$

As mentioned above, $\overrightarrow{\delta L}^n(i,j)$ is a measure of the change in the information $L^n(i,j)$. Let $L^n(i,j)$ be an image smoothness estimator. For this purpose we may use a simple discrete implementation of the Laplacian: $L^n(i,j) = I_{xx}^n(i,j) + I_{yy}^n(i,j)$. Other smoothness estimators might be used, though satisfactory results were already obtained with this very simple selection.

2.1.1.3 How to calculate $\dfrac{\overrightarrow{N}(i,j,n)}{\left|\overrightarrow{N}(i,j,n)\right|}$?

$$\frac{\overrightarrow{N}(i,j,n)}{\left|\overrightarrow{N}(i,j,n)\right|} = \frac{\left(-I_y^n(i,j), I_x^n(i,j)\right)}{\sqrt{\left(I_x^n(i,j)\right)^2 + \left(I_y^n(i,j)\right)^2}} \tag{2.6}$$

$\dfrac{\overrightarrow{N}(i,j,n)}{\left|\overrightarrow{N}(i,j,n)\right|}$ means the isophote direction. We can compute $I_x^n(i,j)$ and $I_y^n(i,j)$ by using some gradient operators (Fig. 2-2)

-1	-1	-1
0	0	0
1	1	1

I_x

-1	0	1
-1	0	1
-1	0	1

I_y

a

-1	-2	-1
0	0	0
1	2	1

I_x

-1	0	1
-2	0	2
-1	0	1

I_y

b

Fig. 2- 2 Some gradient operators. (a) is Prewitt operator. (b) is Sobel operator.

2.1.1.4 How to calculate $\left|\nabla I^n(i,j)\right|$?

$$\left|\nabla I^{n}(i,j)\right| = \begin{cases} \sqrt{\left(I^{n}_{xbm}\right)^2 + \left(I^{n}_{xfM}\right)^2 + \left(I^{n}_{ybm}\right)^2 + \left(I^{n}_{yfM}\right)^2}, when\ \beta^{n} > 0 \\ \sqrt{\left(I^{n}_{xbM}\right)^2 + \left(I^{n}_{xfm}\right)^2 + \left(I^{n}_{ybM}\right)^2 + \left(I^{n}_{yfm}\right)^2}, when\ \beta^{n} < 0 \end{cases}, \quad (2.7)$$

$$\beta^{n}(i,j) = \overrightarrow{\delta L}^{n}(i,j) \cdot \frac{\overrightarrow{N}(i,j,n)}{\left|\overrightarrow{N}(i,j,n)\right|} \quad (2.8)$$

$\left|\nabla I^{n}(i,j)\right|$ stands for the gradient of the image. β^{n} is the projection of $\overrightarrow{\delta L}$ onto the normalized vector $\overrightarrow{N}$, that is, we compute the change of *L* along the direction of $\overrightarrow{N}$. Finally, we multiply β^{n} by a *slope-limited* version of the norm of the gradient of the image. A central differences realization would turn the scheme unstable, and that is the reason for using slope-limiters. The subindexes *b* and *f* denote backward and forward differences respectively, while the subindexes *m* and *M* denote the minimum or maximum. See [27] for details.

2.1.2 Fast Digital Image Inpainting

A fast inpainting algorithm was proposed in [2], based on image diffusion kernels. Let Ω be a small area to be inpainted. The simplest version of the algorithm consists of initializing Ω by clearing its color information and repeatedly convolving the region to be inpainted with a diffusion kernel. It uses a weighted average kernel that only considers contributions from the neighboring pixels. Fig. 2-3 [2] shows the pseudocode of the algorithm and two diffusion kernels.

```
Initialize $\Omega$;
for (iter =0; iter < num_iteration; iter++)
    convolve masked regions with kernel;
```

a	b	a
b	0	b
a	b	a

c	c	c
c	0	c
c	c	c

Fig. 2- 3 (top) Pseudocode for the fast inpainting algorithm. (bottom) Two diffusion kernels used with the algorithm.
a= 0.073235, b = 0.176765, c = 0.125.

Efficiency of the fast inpainting algorithm [2] is two to three orders of magnitude faster than those using partial differential equations. But it constraints the regions to be inpainted must be locally small. If the damaged regions are not small enough, some possibly important information might be discarded. Results might be blurred.

We use the fast inpainting algorithm to inpaint the following pictures. Fig. 2-4 and 2-5 are the examples of inpainting locally small damaged regions. The results look good. Fig. 2-6 is the example of inpainting large damaged regions. The result is blurred.

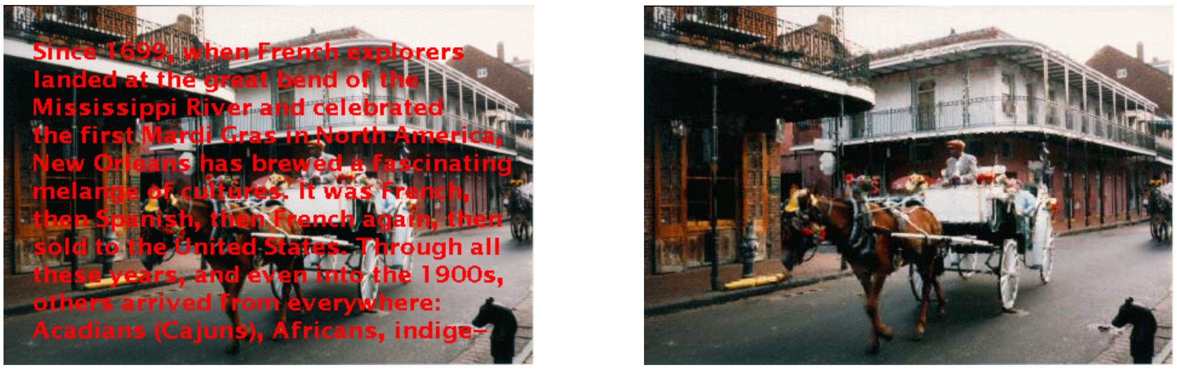

Since 1699, when French explorers
landed at the great bend of the
Mississippi River and celebrated
the first Mardi Gras in North America,
New Orleans has brewed a fascinating
melange of cultures. It was French,
then Spanish, then French again, then
sold to the United States. Through all
these years, and even into the 1900s,
others arrived from everywhere:
Acadians (Cajuns), Africans, indige-

Fig. 2- 4 Removal of subtitles

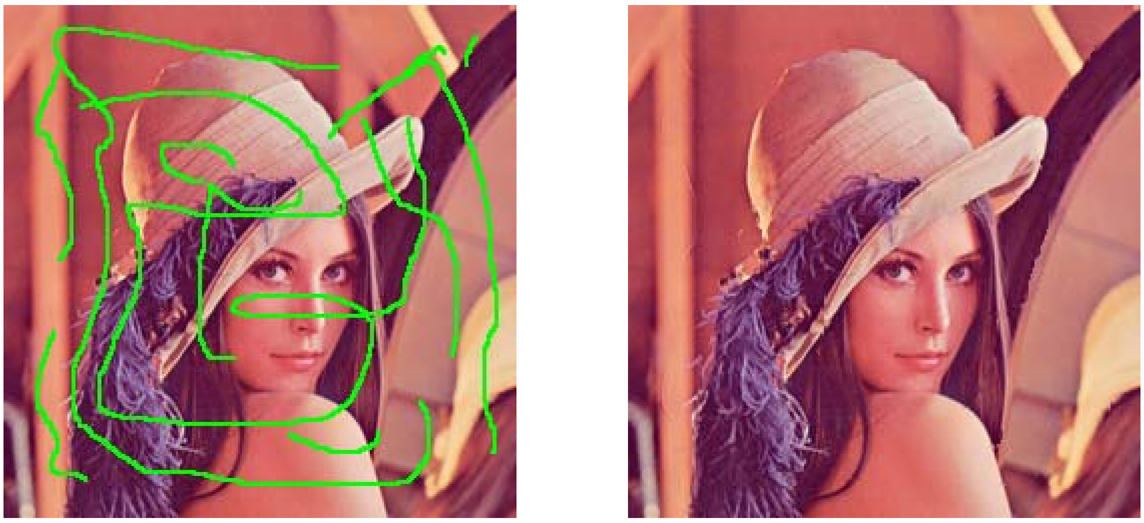
Fig. 2- 5 Lena : (left) Picture with locally small damaged regions. (right) Restored image obtained with fast inpainting algorithm.

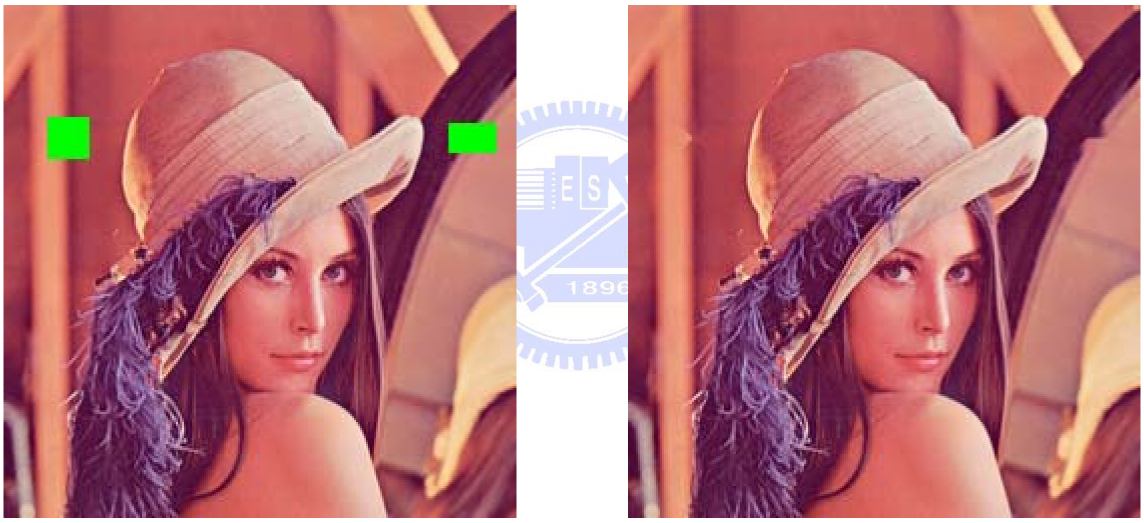
Fig. 2- 6 Lena : (left) Picture with large damaged regions. (right) Restored image obtained with fast inpainting algorithm.

2.1.3 Texture Synthesis

For inpainting large damaged regions well, Efros and Leung et al. [3] proposed an algorithm to solve the problem. In this algorithm, the lost region is filled-in pixel by pixel with the texture from its neighbors. As illustrated in Fig. 2-7 [3], when filling the pixel $p(i,j)$, the algorithm first defines a 3×3 template I_t next to $p(i,j)$, and looks for a $\hat{I}_t$ in the available neighboring blocks such that $d(I_t,\hat{I}_t)$ is minimized, where $d(I_t,\hat{I}_t)$ is defined as the normalized sum of squared differences (SSD) metric (More details can be found in section 2.2). Once the nearest template is found, we copy the pixel (candidate) in the correspondent position to our pixel (current pixel) to be filled-in. Fig. 2-8 shows the algorithm’s results. This algorithm is considerably faster when using the improvements in [10], [18], [19], [20].

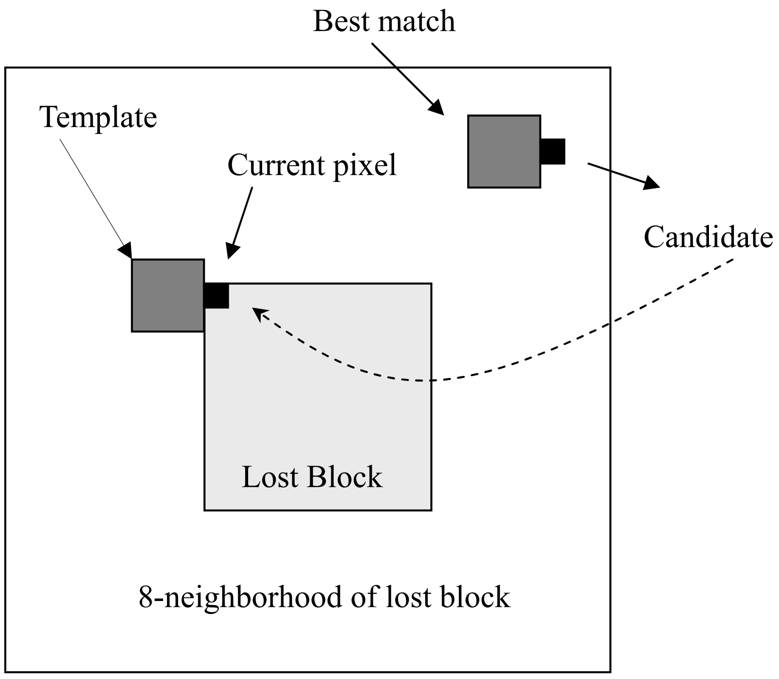

Fig. 2- 7 Texture Synthesis Procedure

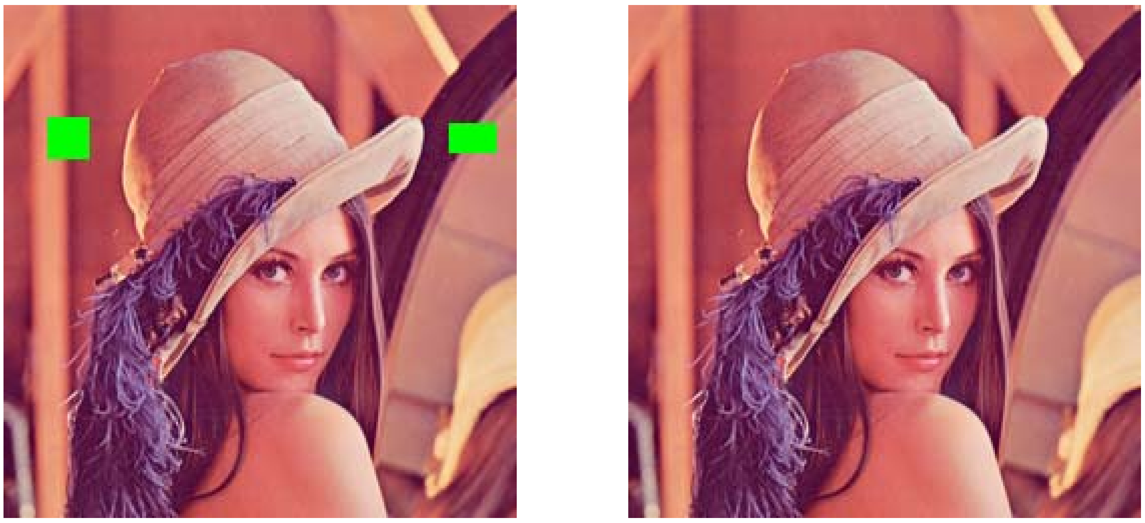
Fig. 2- 8 Lena : (left) Picture with large damaged regions. (right) Restored image obtained with texture synthesis algorithm.

2.1.4 Priority Texture Synthesis

Inspired by the work of Efros and Leung, Criminisi, Pérez and Toyama proposed an exemplar-based texture synthesis algorithm [7] for removing large objects from digital images. Their approach employs an exemplar-based texture synthesis technique modulated by a unified scheme for determining the *fill order* of the target region. Pixels maintain a confidence value, which together with image isophotes, influence their fill priority. Figure 2-9 [6] shows the pseudocode of the algorithm.

The algorithm

```
1. Manually select region $\Omega$ for removal (Fig. 2-10 a)
2. Repeat until region $\Omega$ is empty
    1. Compute boundary $d\Omega$ and priorities P(p)
    2. Propagate texture and structure information
        1. Find patch $\Psi p$ on $d\Omega$ with highest priority P(p) (Fig. 2-10 b)
        2. Find patch $\Psi q$ in $\Phi$ which minimizes SSD($\Psi p$, $\Psi q$) (Fig. 2-10 c)
        3. Copy $\Psi q$ to $\Psi p$ (Fig. 2-10 d)
    3. Update confidence values (More details can be found in section 2.1.4.4)
```

Fig. 2- 9 The pseudocode of the exemplar-based texture synthesis algorithm.

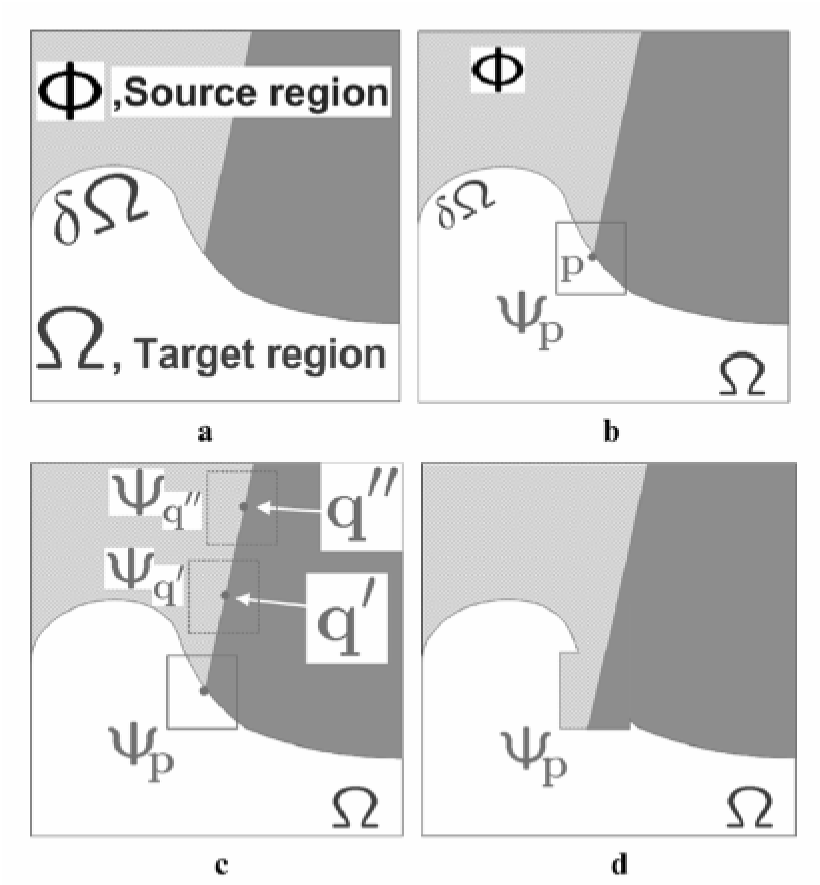

Fig. 2- 10 Structure propagation by exemplar-based texture synthesis.

Fig. 2-10 [7] shows the procedure of structure propagation. (a) Original image, with the target region Ω, its contour $\delta\Omega$, and the source region Φ clearly marked. (b) We want to synthesize the area delimited by the patch Ψp centered on the point $p \in \delta\Omega$. (c) The most likely candidate matches for Ψp lie along the boundary between the two textures in the source region, e.g., $\Psi_{q'}$ and $\Psi_{q''}$. (d) The best-matching patch in the candidates set has been copied into the position occupied by Ψp, thus achieving partial filling of Ω. Notice that both texture and structure (the separating line) have been propagated inside the target region. The target region Ω has, now, shrunken and its front $\delta\Omega$ has assumed a different shape.

2.1.4.1 How to calculate P(p)?

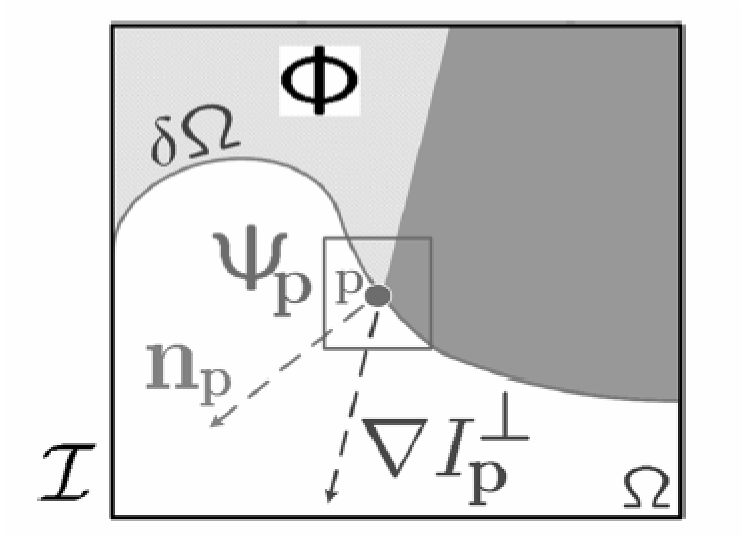

Fig. 2- 11 Notation diagram.

Fig. 2-11 shows the notation diagram [7]. Given a patch Ψq centered at the point p for some $p \in d\Omega$, n_p is the normal to the contour $\delta\Omega$ of the target region Ω and $\nabla I_p^{\perp}$ is the isophote (direction and intensity) at point p. The entire image is denoted with I. We define its priority P(p) as the product of two terms P(p) = C(p) D(p), We call C(p) the *confidence* term and D(p) the *data* term, and they are defined as follows:

$$C(p) = \frac{\sum_{q \in \Psi p \cap (\mathrm{I} - \Omega)} C(q)}{|\Psi p|} \tag{2.9}$$

$$D(p) = \frac{|\nabla I_p^{\perp} \cdot n_p|}{\alpha} \tag{2.10}$$

where is |Ψp | the area of Ψp, α is a normalization factor (e.g., α = 255 for a typical grey-level image), n_p (More details can be found in section 2.1.4.2) is a unit vector orthogonal to the front dΩ in the point p, and $\perp$ (More details can be found in section 2.1.4.3) denotes the orthogonal operator. The priority P(p) is computed for every border patch, with distinct patches for each pixel on the boundary of the target region. During initialization, the function C(p) is set to C(p) = 0 $\forall p \in \Omega$ and C(p) = 1 $\forall p \in \mathrm{I} - \Omega$.

2.1.4.2 How to calculate n_p ?

Given a point p∈dΩ, the normal direction n_p is computed as follows : 1) the positions of the "control" points of dΩ are filtered via a bidimensional Gaussian kernel (Fig. 2-12) and, 2) n_p is estimated as the unit vector orthogonal to the line through the preceding and the successive points in the list. Alternative implementation may make use of curve model fitting [23].

0	-1	0
0	2	0
0	-1	0

Gx

0	0	0
-1	2	-1
0	0	0

Gy

Fig. 2- 12 A bidimensional Gaussion Kernel filter

2.1.4.3 How to calculate $\nabla I_p^{\perp}$?

$\nabla I_p^{\perp}$ denotes the orthogonal gradient vector. The gradient ∇I_p is computed as the maximum value of the image gradient in $\Psi p \cap \mathrm{I}$. Robust filtering techniques may also be employed here, such as using some gradient operators (Fig. 2-13). After computing ∇I_p, (-Gy, Gx) is the orthogonal gradient vector $\nabla I_p^{\perp}$.

-1	-1	-1
0	0	0
1	1	1

Gx

-1	0	1
-1	0	1
-1	0	1

Gy

a

-1	-2	-1
0	0	0
1	2	1

Gx

-1	0	1
-2	0	2
-1	0	1

Gy

b

Fig. 2- 13 Some gradient operators. (a) is Prewitt operator. (b) is Sobel operator.

2.1.4.4 How to update confidence value ?

After the patch $\Psi_{\hat{p}}$ has been filled with new pixel values, the confidence C(p) is updated in the area delimited by $\Psi_{\hat{p}}$, as follows:

$$C(p) = C(\hat{p}), \quad \forall p \in \Psi_{\hat{p}} \cap \Omega \tag{2.11}$$

This simple update rule allows us to measure the relative confidence of patches on the fill front without image-specific parameters. As filling proceeds, confidence values decay, indicating that we are less sure of the color values of pixels near the center of the target region.

2.2 Block Matching

The block matching problem is one that occurs in various fields of applications, such as the image processing, multimedia and vision fields. The basic idea for solving the block matching problem is to minimize some measure of similarity between a template block of pixels in the current image to all candidate blocks in the reference image within a given search range. In this section, we will describe a new algorithm [10] for solving the block matching problem which is independent of image content and is faster than other full-search methods.

2.2.1 SAD and SSD

We first introduce two most popular similarity measures. They are defined as :

$$SAD_{(u,v)} = \sum_{j=0}^{B-1}\sum_{i=0}^{B-1}\left| f_t(i,j) - f_{t-1}(i+u, j+v)\right| \tag{2.12}$$

$$SSD_{(u,v)} = \sum_{j=0}^{B-1}\sum_{i=0}^{B-1}\left(f_t(i,j) - f_{t-1}(i+u, j+v)\right)^2 \tag{2.13}$$

SAD means the sum of absolute difference and SSD means the sum of squared difference. *B* is a block size and (u, v) is a displacement vector for a candidate block relative to the template block. Lets compare the difference between SAD (2.12) and SSD (2.13). Because of its lack of multiplications, the SAD metric is far more convenient for use in hardware designs, and is therefore used almost exclusively. However, minimizing the SSD metric corresponds to maximizing the PSNR (More details can be found in section 2.3). If a maximum PSNR is desired, SSD should be the metric of choice. Therefore, we choose SSD metric to measure similarity when texture synthesizing.

2.2.2 The FFT Block Matching Algorithm

Steven L. Kilthau, Mark S. Drew, and Torsten Möller et al. [10] proposed an FFT Block matching algorithm. It is faster than other full-search methods. In order to maximize the PSNR, the algorithm minimizes the SSD metric given in Eq.2.13. Following a trivial expansion, the mathematical definition of the per-block computation is given by:

$$\min_{\forall u,v} \sum_{j=0}^{B-1} \sum_{i=0}^{B-1} \left[f_t(i,j)^2 + f_{t-1}(i+u,j+v)^2 - 2 f_t(i,j) f_{t-1}(i+u,j+v) \right] \quad (2.14)$$

Since the term $f_t(i,j)^2$ appears across the entire minimum, it can be removed from the sum without affecting the resulting solution. Removing this term and separating the sum leaves us with the following equation:

$$\min_{\forall u,v} \sum_{j=0}^{B-1} \sum_{i=0}^{B-1} f_{t-1}(i+u,j+v)^2 - 2 \sum_{j=0}^{B-1} \sum_{i=0}^{B-1} f_t(i,j) f_{t-1}(i+u,j+v) \quad (2.15)$$

Finally, we employ a novel data structure called the Windowed-Sum-Squared-Table and use the fast Fourier transform (FFT) in its computation of the sum squared difference (SSD) metric. Figure 2-14 shows the three basic steps of the FFT Block Matching algorithm.

The Algorithm

1. Resize input image to include a zero pad
   (More details can be found in section 2.2.2.1)
2. Compute the windowed sum squared table
   (More details can be found in section 2.2.2.2)
3. Compute a per-block convolution sum
   (More details can be found in section 2.2.2.3)

Fig. 2- 14 FFT Block Matching algorithm.

2.2.2.1 Resize input image to include a zero pad

Given a search range of ±P we apply a zero pad of P pixels around the entire image. This simple preprocess eliminates the need for conditionals within the innermost loops of our algorithm and greatly increases its speed. In other words, it is simply to allow convenient calculation of the SSD metric without using conditionals for those search locations that lie outside of the dimensions of the original image.

2.2.2.2 Windowed Sum Squared Table

We use a variant of the well known summed area table (SAT), introduced in [24]. Given an input image f, a summed area table is a new image f_{SAT} such that

$$f_{SAT}(i,j)=\Sigma_{k\le i}\Sigma_{l\le j}\, f(k,l) \qquad (2.16)$$

Summed area tables can be very easily computed by applying the following recurrence, being careful to set $f(i,j)$ to zero when either of the indices is negative:

$$f_{SAT}(i,j)=\left[f(i,j)+f_{SAT}(i-1,j)+f_{SAT}(i,j-1)-f_{SAT}(i-1,j-1)\right] \quad (2.17)$$

Fig. 2-15 is a simple example for computing SAT.

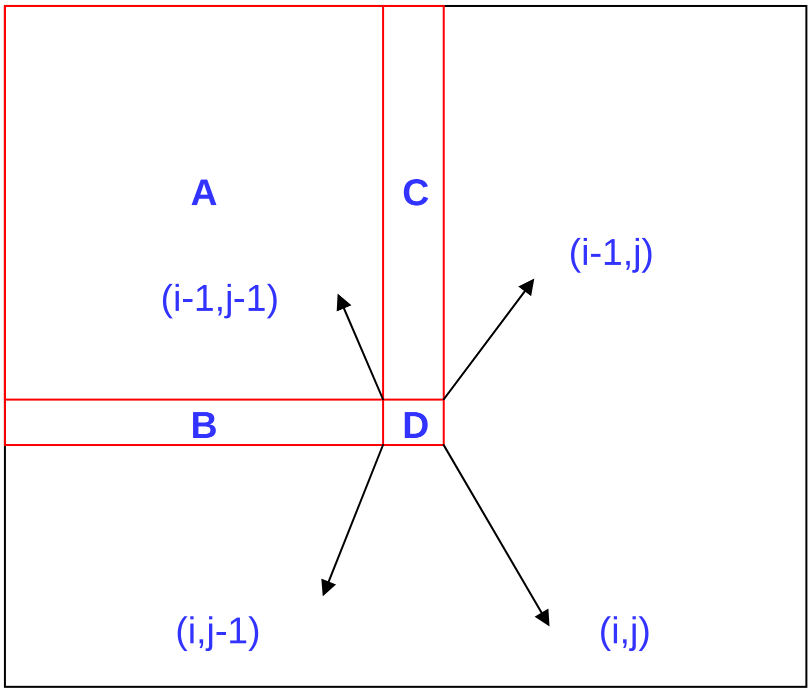

Fig. 2- 15 A simple example for computing SAT.

$$f_{SAT}(i,j) = f(i,j) + (A+C) + (A+B) - A = D + A + B + C$$

The WSST differs from the SAT in that each pixel needs to represent a *sum of squares*, where the sum extends only over the last $B \times B$ sub-image (window), with B the block size.

$$f_{SST}(i,j) = \left[f(i,j)^2 + f_{SST}(i-1,j) + f_{SST}(i,j-1) - f_{SST}(i-1,j-1) \right] \quad (2.18)$$

$$f_{WSST}(i,j) = \sum_{s=j-B+1}^{j} \sum_{t=i-B+1}^{i} f(s,t)^2 =$$
$$\left[f_{SST}(i,j)\right] + \left[f_{SST}(-1,j) - f_{SST}(i-B,j)\right] + \left[f_{SST}(i,-1) - f_{SST}(i,j-B)\right] +$$
$$\left[f_{SST}(-1,-1) + f_{SST}(i-B,j-B) - f_{SST}(i-B,-1) - f_{SST}(-1,j-B)\right] \quad (2.19)$$

2.2.2.3 Per-Block Convolution Sum

We show that computation of the second term in Eq.2.15 amounts to the evaluation of a correlation sum for each template block, which we evaluate as a convolution sum.

$$\sum_{j=0}^{B-1} \sum_{i=0}^{B-1} f_t(i,j)\, f_{t-1}(i+u, j+v) \quad (2.20)$$

In order to efficiently compute the correlation, we will convert it to a convolution (Eq.2.20) and then use the Fast Fourier transform. For each template block, we create two images of size *(2P+B)*(2P+B)*. The first image, *template* , corresponds to the template block and is computed by simply multiplying the block by 2, reversing the pixels, and zero padding to the correct size. The pixel reversal effectively changes the correlation sum into an equivalent convolution sum. The second image, *candidates* , corresponds to the square containing all pixels of all candidate blocks in the search range. This square can be copied directly from the reference image. Given these two images, we can compute a new image, *result* , according to the following formula:

$$\sum_{j=0}^{B-1}\sum_{i=0}^{B-1} f_t(i,j)\, f_{t-1}(i+u,j+v) = result = FFT^{-1}\left(FFT(template)\bullet FFT(candidates)\right) \quad (2.21)$$

2.3 PSNR

Signal-to-noise (SNR) measures are estimates of the quality of reconstructed images compared with their original images. The basic idea is to compute a single number that reflects the quality of a reconstructed image. Reconstructed images with higher metrics are judged better. The actual metric we will compute is the peak-signal-to-reconstructed image measure which is called PSNR. The higher measures might mean better quality. Assume we are given a source image f(i,j) that contains N by N pixels and a reconstructed image F(i,j) which is reconstructed by inpainting a damaged version of f(i,j). The pixel values f(i,j) range between black (0) and white (255). We compute the mean squared error (MSE) of the reconstructed image as follows :

$$MSE=\frac{\sum[f(i,j)-F(i,j)]^2}{N^2} \quad (2.22)$$

The root mean squared error (RMSE) is the square root of MSE :

$$RMSE=\sqrt{\frac{\sum[f(i,j)-F(i,j)]^2}{N^2}}=\sqrt{MSE} \quad (2.23)$$

PSNR in decibels (dB) is computed as follows:

$$PSNR = 10\log(\frac{255^2}{MSE}) \tag{2.24}$$

2.4 Mathematical Morphology

Mathematical morphology is a tool for extracting image components that are useful in the representation and description of region shapes, such as boundaries, skeletons, and convex hulls. Mathematical morphology is a set-theoretic method. Sets in mathematical morphology represent the shapes of objects in an image. The operations of mathematical morphology were originally defined as set operations and shown to be useful for image processing.

In general, morphological approach is based upon binary images. In binary images, each pixel can be viewed as an element in Z^2. Gray-scale digital images can be represented as sets whose components are in Z^3, two components are the coordinates of a pixel, and the third corresponds to its discrete intensity value. The morphological operations input a source image and a structuring element which is another image usually smaller than the source image. The structuring element is a predetermined geometric shape, and there are some common structuring elements as shown in Fig. 2-16.

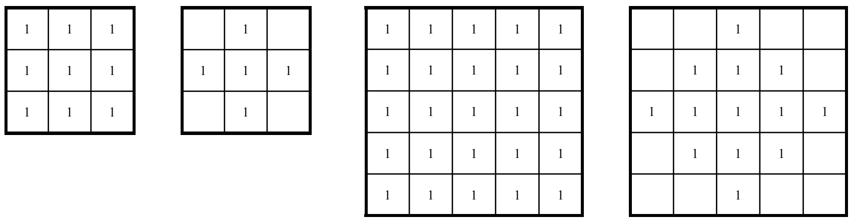

Fig. 2- 16 Examples of structuring elements

Here, we will discuss morphological operators in binary images [25, 26]. Given a source image *A* and a structuring element *B* in Z^2.

2.4.1 Basic definition

The *Translation* of *A* by the point *x* in Z^2, denoted $A_{\vec{x}}$, is defined by

$$A_{\vec{x}} = \{\vec{a} + \vec{x} \mid \forall \vec{a} \in A\} = A + \vec{x} \tag{2.25}$$

where the plus sign refers to vector addition.

And the *Reflection* of *B*, denoted $\hat{B}$, is defined as

$$B = \{-\vec{b} \mid \vec{b} \in B\} \tag{2.26}$$

The examples of *Translation* and *Reflection* are shown in Fig. 2-17.

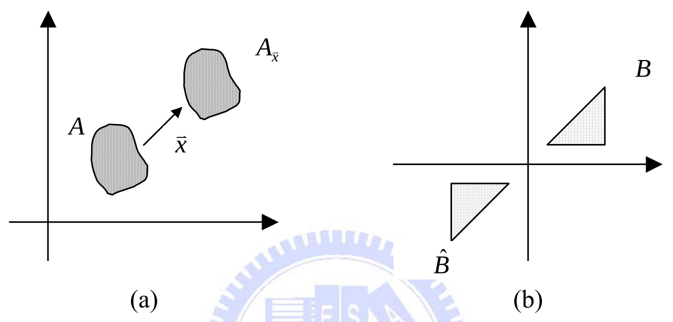

Fig. 2- 17 Examples of (a) *Translation* and (b) *Reflection*

2.4.2 Morphological operations

Here, we introduced two of the fundamental morphology operations：Dilation and Erosion used in binary images, and introduced two operators：Closing and opening that extended from Dilation and Erosion.

2.4.2.1 Dilation and Erosion

The *Dilation* of *A* by *B*, denoted $D_B(A)$, is defined as

$$D_B(A) = A \oplus \hat{B} = \{\vec{x} \mid \hat{B} + \vec{x} \cap A \neq \phi\} \tag{2.27}$$

Where B is the structuring element.

And the *Erosion* of A by B, denoted $E_B(A)$, is defined as

$$E_B(A) = A \ominus B = \{\vec{x} \mid B + \vec{x} \subset A\} \tag{2.28}$$

The examples of *Dilation* and *Erosion* are shown in Fig. 2-18 (c) and (d). The dilation of *A* by *B* is the set of all $\vec{x}$ displacements such that $\hat{B}$ and *A* overlap by at least one nonzero element. The erosion of *A* by *B* is the set of all points $\vec{x}$ such that *B* translated by $\vec{x}$ is contained in *A*.

2.4.2.2 Closing and Opening

The *Closing* of set *A* by structuring element *B*, denoted $C_B(A)$, is defined as

$$C_B(A) = A \bullet B = E_{\hat{B}}(D_B(A)) = (A \oplus \hat{B}) \ominus \hat{B} \qquad (2.29)$$

And the *Opening* of set *A* by structuring element *B*, denoted $O_B(A)$, is defined as

$$O_B(A) = A \circ B = D_{\hat{B}}(E_B(A)) = (A \ominus B) \oplus B \qquad (2.30)$$

The examples of *Closing* and *Opening* are shown in Fig. 2-18 (e) and (f). The closing of *A* by *B* is simply the dilation of *A* by *B*, followed by the erosion of the result by $\hat{B}$. The opening of *A* by *B* is simply the erosion of *A* by *B*, followed by the dilation of the result by $\hat{B}$.

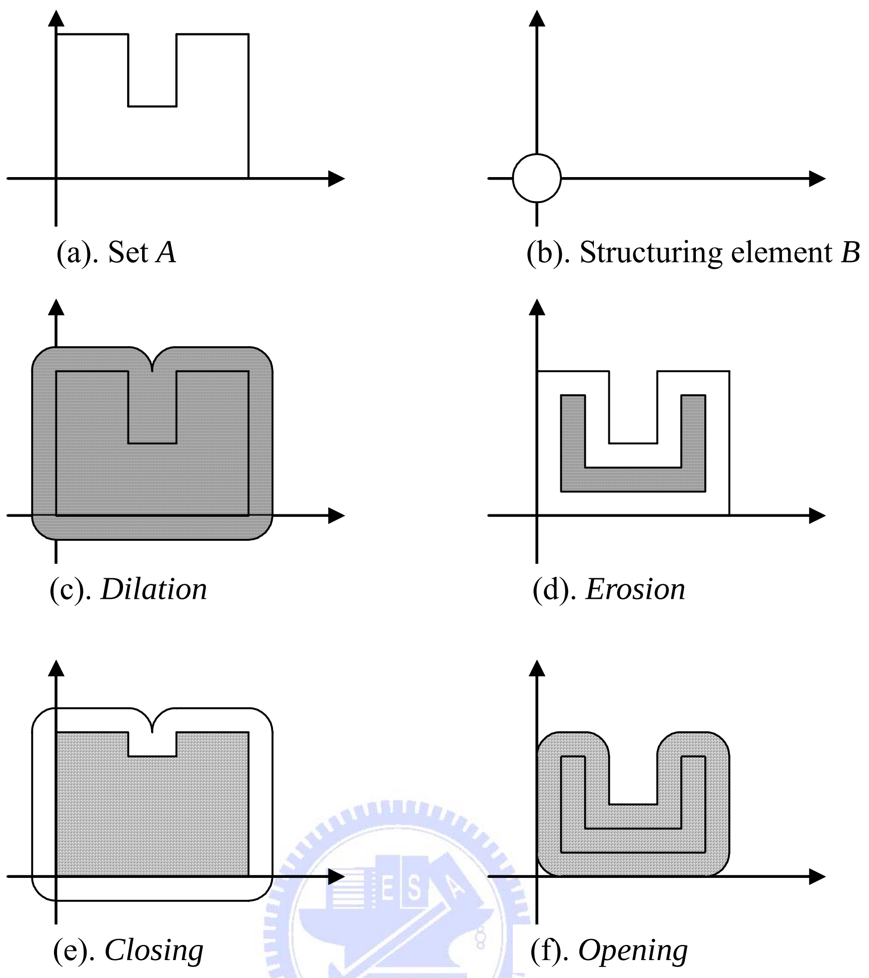

Fig. 2- 18 (a). Set *A*. (b) Structuring element *B*.
(c). The *Dilation* of *A* by *B*. (d). The *Erosion* of *A* by *B*.
(e). The *Closing* of *A* by *B*. (f). The *Opening* of *A* by *B*.

2.4.3 Extension to Gray-Scale Images

In this section we extend to gray-level images the basic operations of dilation, and erosion. Throughout the discussions that follow, we deal with digital image functions of the forms $f(x,y)$ and $b(x,y)$, where $f(x,y)$ is the gray-scale image and $b(x,y)$ is a structuring element.

Gray-Scale dilation of f by b, denoted by $f \oplus b$, is define as：

$$(f \oplus b)(s,t) = \max\{ f(s-x,t-y) + b(x,y) \,|\, (s-x),(t-y) \in D_f ; (x,y) \in D_b \} \qquad (2.31)$$

Where D_f and D_b are the domain of f and b, respectively. As before, b is the structuring element of the morphological process but note that b is now a function rather than a set. Because dilation is based on choosing the maximum value of $f + b$ in a neighborhood defined by the shape of the structuring element, the general effect of performing dilation on a gray-scale image is two-fold: (1) if all the values of the structuring element are positive, the output image tends to be brighter than the input; and (2) dark details either are reduced or eliminated, depending on how their values and shapes relate to the structuring element used for dilation. As illustrated in Fig 2-19 (b).

Gray-scale erosion of f by b, denoted by $f \ominus b$, is define as：

$$(f \ominus b)(s,t) = \min\{ f(s+x, t+y) - b(x,y) \,|\, (s+x),(t+y) \in D_f; (x,y) \in D_b \} \qquad (2.32)$$

Where D_f and D_b are the domain of f and b. Because erosion is based on choosing the minimum values of $f - b$ in a neighborhood defined by the shape of the structuring element, the general effect of performing erosion on a gray-scale image is two-fold: (1) if all the values of the structuring element are positive, the output image tends to be darker than the input; and (2) bright details are reduced or eliminated, depending on the used structuring element. As illustrated in Fig 2-19 (c).

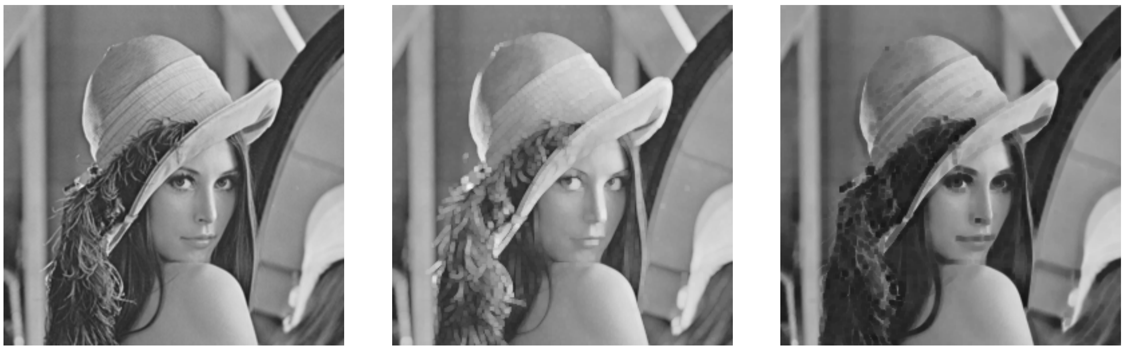

Fig. 2- 19 (a) The original of Lena image
(b) Dilation of Lena image
(c) Erosion of Lena image

The usage of closing and closing is to smooth contours of objects. In gray-level images, closing is used for brighter objects with darker background, and opening is used for darker object objects with brighter background. As illustrated in Fig 2-20 (b) and (c).

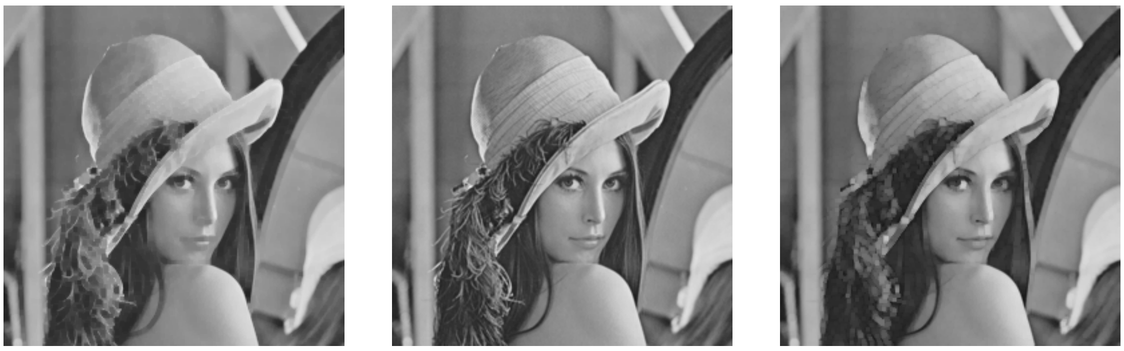

(a) (b) (c)

Fig. 2- 20 (a) The original of Lena image
(b) Closing of Lena image
(c) Opening of Lena image

2.4.4 Morphological Gradient

The Morphological Gradient of an image, denoted G:

$$G = D_B(A) - E_B(A) = (A \oplus B) - (A \ominus B) \tag{2.33}$$

or

$$G = D_B(A) - A = (A \oplus B) - A \tag{2.34}$$

or

$$G = A - E_B(A) = A - (A \ominus B) \tag{2.35}$$

The morphological gradient highlights sharp gray-scale transitions in the source image. In other words, morphological gradient can extract the boundary of an object. However, the morphological gradient is sensitive to the shape of the chosen structuring element. Here are examples of dilation, erosion, closing, opening, and morphological gradient of the gray-scale image, Lena, with the 3×3 structuring element as shown in Fig 2-21.

(a)

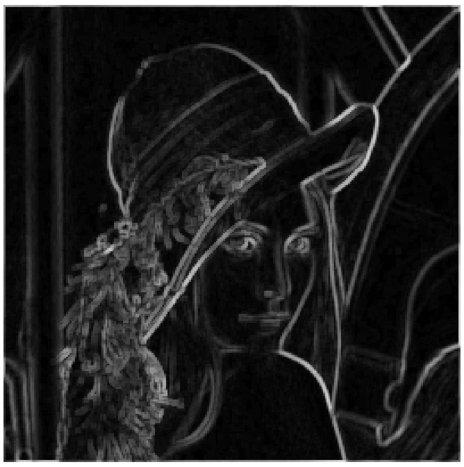
(b)

Fig. 2- 21 (a) The original of Lena image

(b) Morphological gradient of Lena image

CHAPTER 3
The Proposed Method

In this chapter, we will introduce the architecture of the inpainting system based on the proposed method. We focus on these images with several small and large damaged regions, such as the image shown in Fig. 3-1. The goal of this paper is to effectively and correctly inpaint these damaged images. It is known that "Fast Digital Image Inpainting" [2] can fast inpaint small damaged regions, but it can't work well for large damaged regions. "Priority Texture Synthesis" [7] can both inpaint small and large damaged regions well, but it spend too much time. Therefore, we propose a new inpainting method that will combine "Fast Digital Image Inpainting" and "Priority Texture Synthesis". In section 3.1, we will discuss the process of our image inpainting. In section 3.2, we will utilize morphological operations to automatically split the damaged regions into several small and large parts. In section 3.3, we will modify the "Fast Digital Image Inpainting" algorithm and then apply it to inpaint these small damaged parts. In section 3.4, we will apply the "Priority Texture Synthesis" algorithm to inpaint these large damaged parts and add the FFT block matching algorithm to speedup the time of searching similar textures. Finally, we will summarize the proposed method in Section 3.5.

3.1 Overview of Our Image Inpainting System

We designed a simple drawing interface, which allows users to draw lines or surfaces. Users need to input a damaged image at the start of the inpainting process. As illustrated in Fig. 3-2, when users mark these damaged regions from the input image, the system will split the damaged regions into several small and large parts according to the structuring element which users set up. Then the system will show the splitting result. If we don't satisfy the splitting result, we can re-set up the structuring element to split the damaged regions.

After splitting these damaged regions, the system will automatically use “Fast Digital Image Inpainting” to inpaint small damaged parts and use “Priority Texture Synthesis” to inpaint large damaged parts. At last, the system will not only show the reconstructed result but also show several intermediate steps of the reconstruction on the interface.

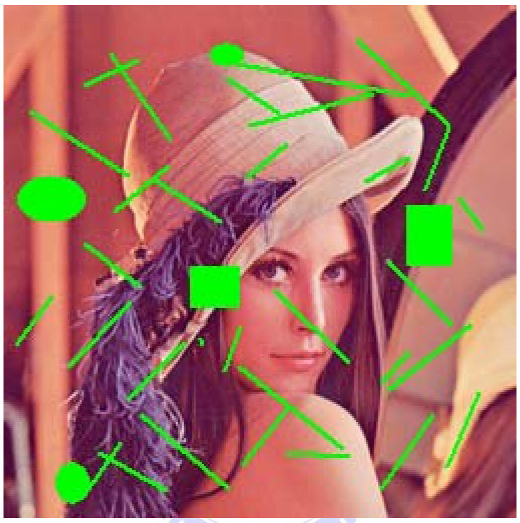

Fig. 3- 1 A lena image with several small and large damaged regions

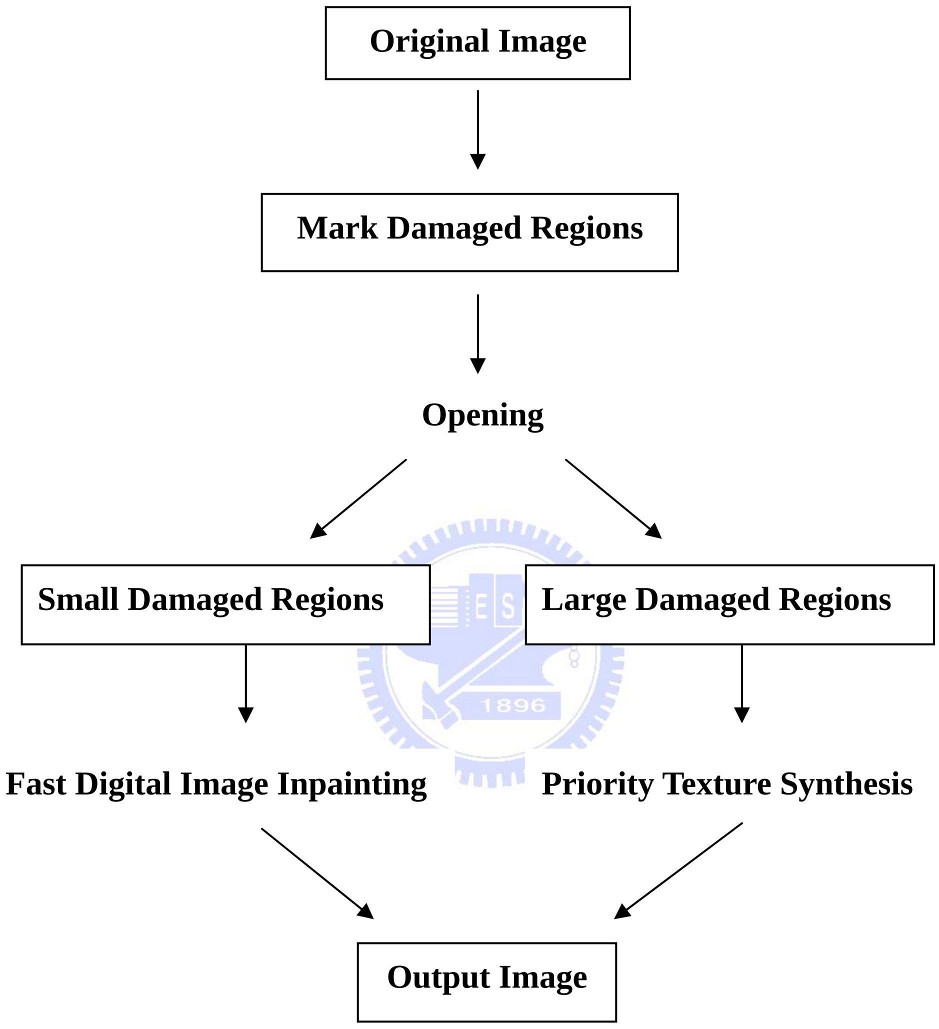

Fig. 3- 2 Overview of Our Image Inpainting System

3.2 Splitting the damaged regions into several small and large parts

Morphologigical operators are attractive because they involve simple logical operations and can be easily implemented. A fundamental feature of mathematical morphology is the use of a structuring element. This is essentially a smaller version of the input image, and contains structure of the type that is to be analyzed in the image. The two basic morphological operators are dilation and erosion. Dilation expands (for binary image) and brightens (for gray-scale image) an image, while erosion shrinks and darkens. Dilation is performed by sliding the structuring element over the image while adding the values of the structuring element to the image, and then recording the maximum value reached at each point. Erosion is similar, except that the structuring element values are subtracted from the image, and the global minimum is taken.

The opening operation is created by first eroding and then dilating an image. Physically, the binary opening operation extracts some shapes whose sizes are larger enough than the structuring element. As illustrated in Fig. 3-3, there are some shapes numbered from 1 to 6. After opening, we see that this operation extracts shape 5, 6 and discards shape 1, 2, 3, 4. Fig. 3-4 is an opening operation example for a binary image. It extracts the shapes whose sizes are larger than 9*9 window size according to 9*9 structuring element.

Viewing from another angle, we can apply the opening operation to split the damaged regions into several small and large parts according to the structure element for our test images. There are two examples. Fig. 3-5 (b) splits the damaged regions into two parts by using “opening” according to 3*3 structuring element. “Green” represents small damaged parts and “Blue” represents large damaged parts. Similarly, Fig. 3-6 (b) splits the damaged regions into two parts by using “opening” according to 3*3 structuring element. “Yellow” represents small damaged parts and “Blue” represents large damaged parts.

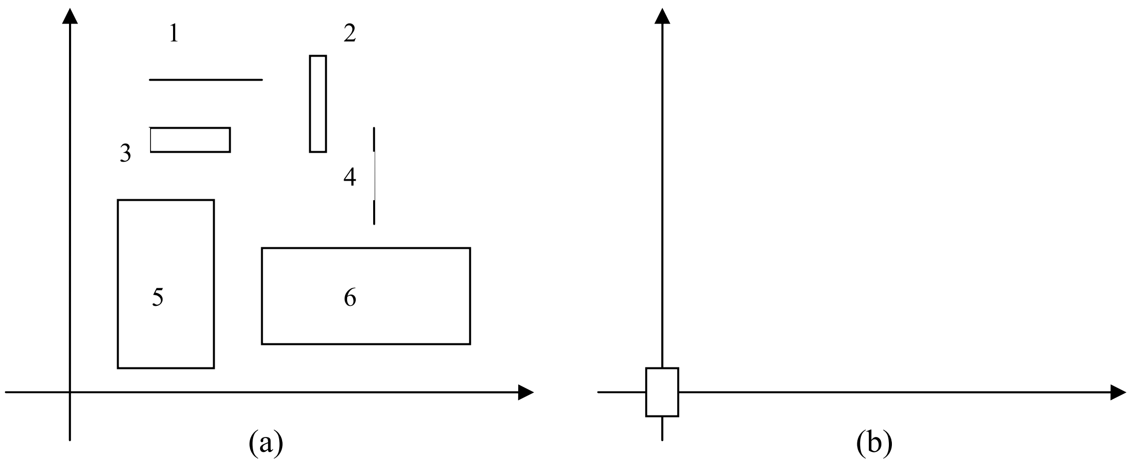

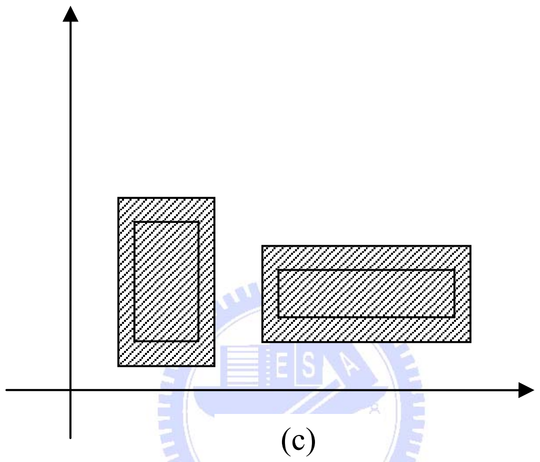

Fig. 3- 3 (a) Set *A* (b) Structuring element *B* (c) The *Opening* of *A* by *B*.

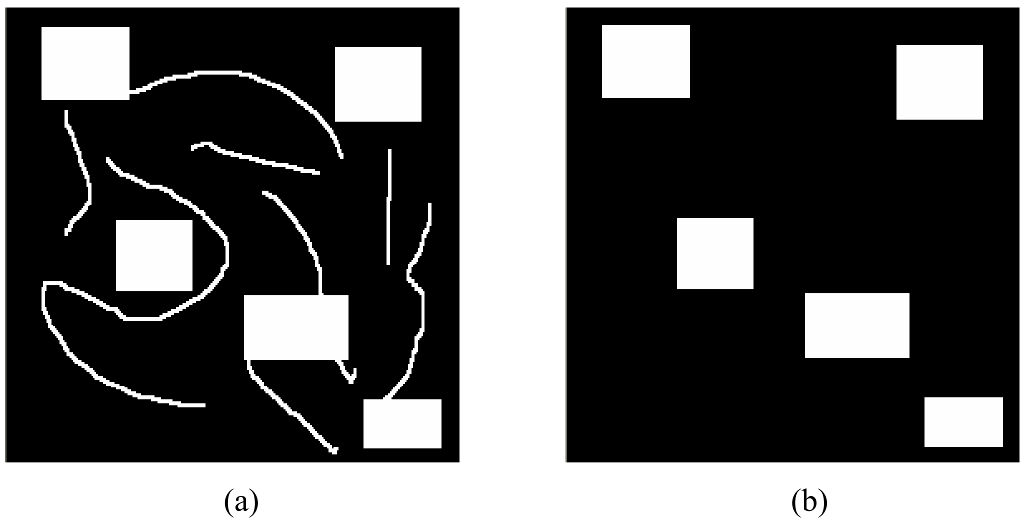

Fig. 3- 4 (a) A binary image : *A* (b) The *Opening* of *A* by 9*9 structuring element.

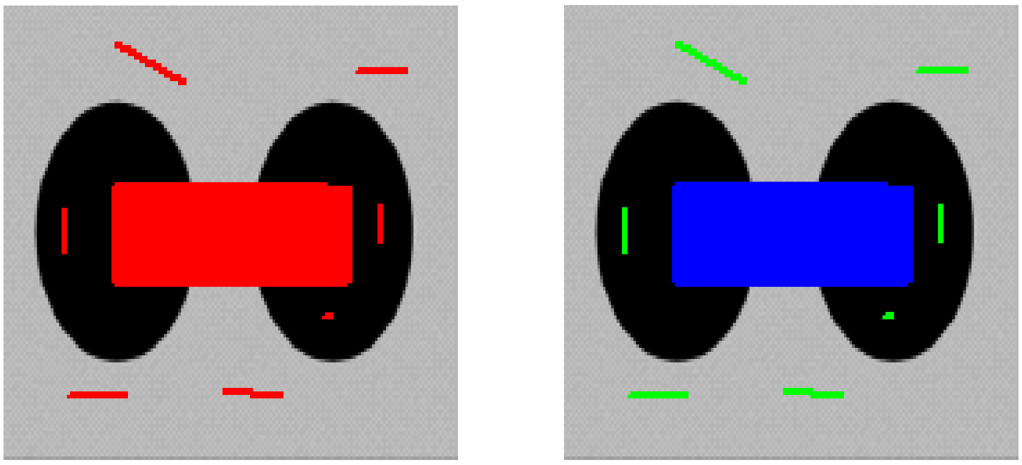

(a) (b)

Fig. 3- 5 (a) A damaged elliptic image (b) Splits the damaged regions into two parts

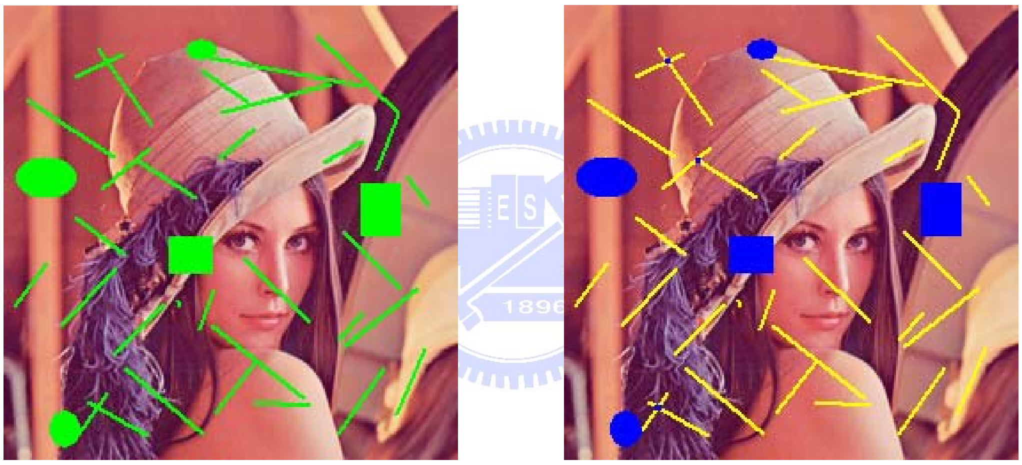

(a) (b)

Fig. 3- 6 (a) A damaged lena image (b) Splits the damaged regions into two parts

3.3 Using "Fast Digital Image Inpainting" to inpaint these small damaged parts

The fast inpainting algorithm can faster inpaint the locally small damaged regions well than other methods. Here, we modify the "Fast Digital Image Inpainting" algorithm and let it be more performance. The new algorithm doesn't setup iterative-times. We will apply it to inpaint these small damaged parts after splitting. The modification of this algorithm is described as below：

The new algorithm

```
1. After splitting, the algorithm automatically selects these small damaged regions $\Omega$.
2. Repeat until region $\Omega$ is empty
    2.1. Mark boundary $d\Omega$.
    2.2. For each boundary pixel, compute the average of its undamaged
         neighborhood pixels, and then copy it to the boundary pixel.
    2.3. Update these small damaged regions $\Omega$
```

Fig. 3- 7 The pseudocode of the algorithm

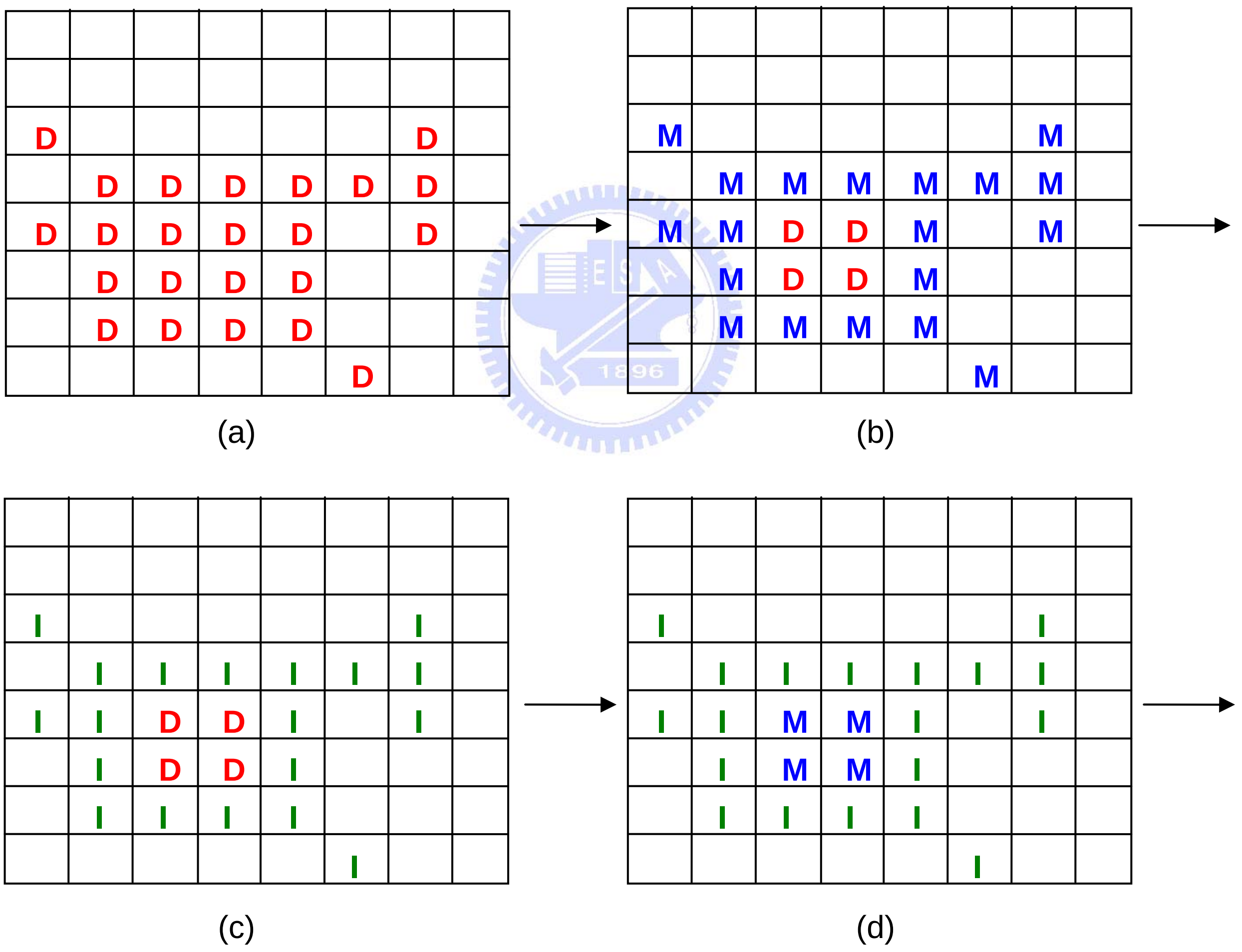

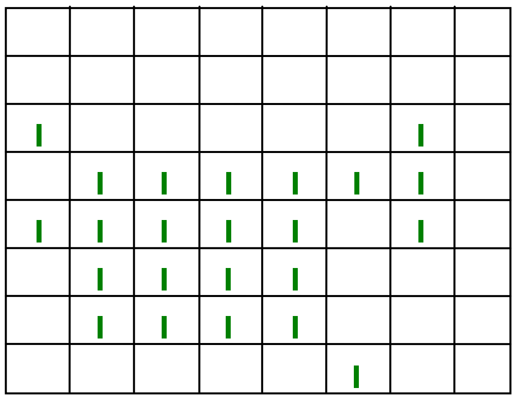

(e)

Fig. 3- 8 The step by step example shows how the algorithm inpaints these small damaged regions.

Let us see an example. As illustrated in Fig. 3-8, the algorithm first selects these small damaged regions Ω "Red D" (Fig. 3-8. a). Because Ω is not empty, the algorithm marks the boundary $d\Omega$ "Blue M" (Fig. 3-8. b). For each "Blue M", compute the average of its undamaged neighboring pixels, and then copy it to the boundary pixel. "Green I" represents the region which has been inpainted (Fig. 3-8. c). The algorithm updates the damaged regions Ω, and then repeats previous steps untill Ω is empty (Fig. 3-8. d and 3-8. e). Our test images are shown in Fig. 3-9 and 3-10.

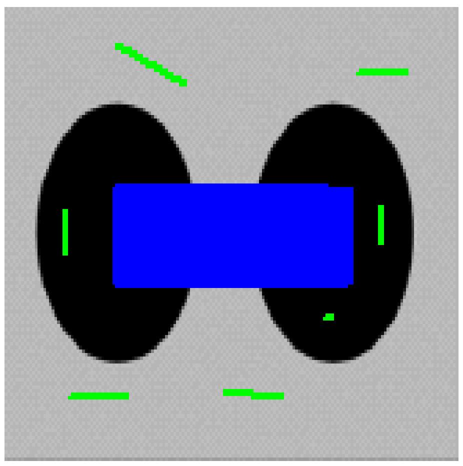
(a)

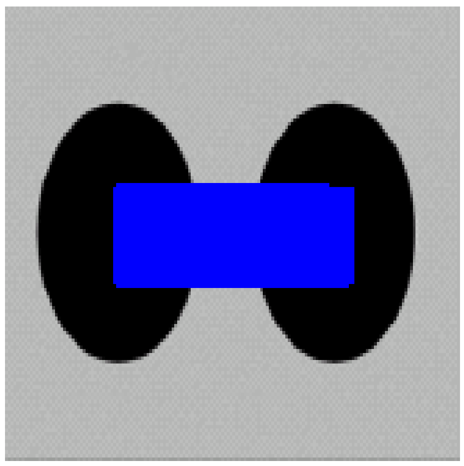
(b)

Fig. 3- 9 (a) A Splitted elliptic image (b) The small damaged parts “Green” has been inpainted well by this algorithm.

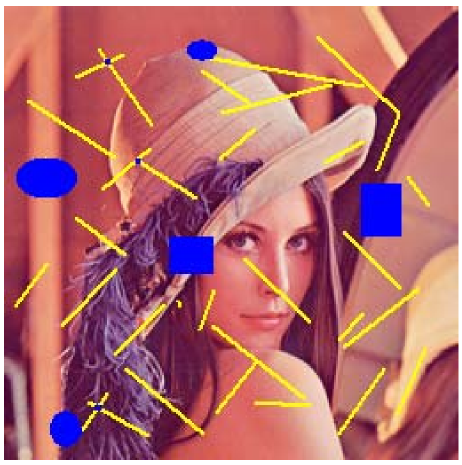
(a)

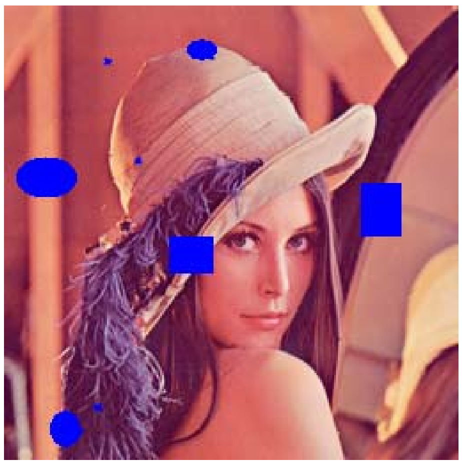
(b)

Fig. 3- 10 (a) A Splitted lena image (b) The small damaged parts “Yellow” has been inpainted well by this algorithm.

3.4 Using “Priority Texture Synthesis” to inpaint these large damaged parts

After inpainting these small damaged regions, there only remains the larged damaged regions. The “priority texture synthesis” algorithm can efficiently and correctly inpaint the large damaged regions. Therefore, we will apply it to inpaint these large damaged parts. At the same time, we will also add the FFT block matching algorithm from section 2.2.2 to speedup the time of searching similar textures. Our test images are shown in Fig. 3-11 and 3-12.

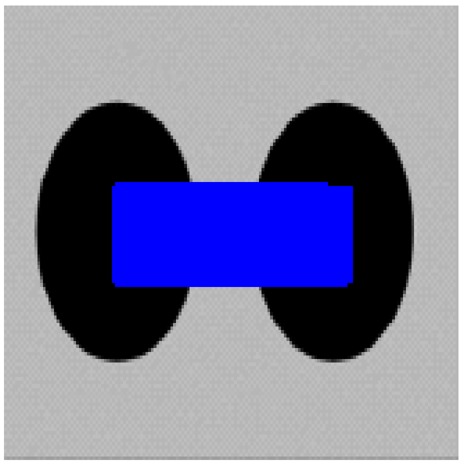
(a)

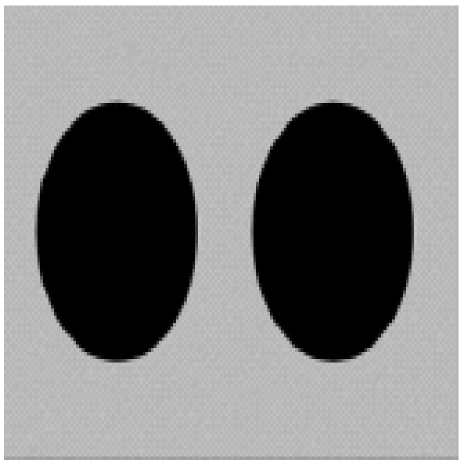
(b)

Fig. 3- 11 (a) An elliptic image followed by Fig. 3-9. b (b) The large damaged parts "Blue" has been inpainted well by priority texture synthesis.

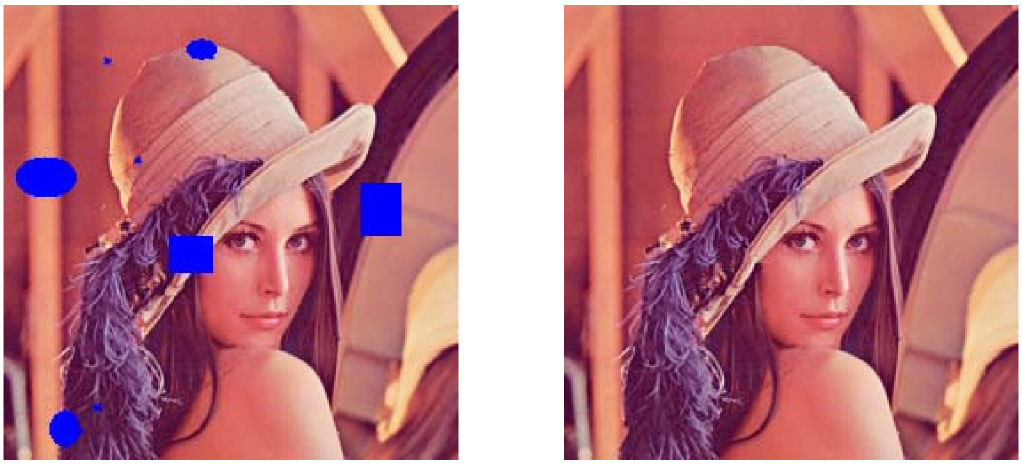
(a) (b)

Fig. 3- 12 (a) A lena image followed by Fig. 3-10. b (b) The large damaged parts "Blue" has been inpainted well by priority texture synthesis.

3.5 Summation

The proposed method combines "Fast Digital Image Inpainting" and "Priority Texture Synthesis" to inpaint the damaged images. The procedure first uses "opening" to split the damaged regions into several small and large parts. After splitting, it will automatically use "Fast Digital Image Inpainting" to inpaint small damaged parts and use "Priority Texture Synthesis" to inpaint large damaged parts. Experimental results indicate that our method can not only inpaint these damaged images well but also efficiently save computational time. More experimental results and comparisons are shown in Chpater 4.

CHAPTER 4
Experimental Results

In this chapter, we will present more experimental results and comparisons obtained by applying the proposed method described in chapter 3. In section 4.1, we will introduce our experiment environment. Experimental results and comparisons are shown in section 4.2.

4.1 Experimental Environment

In this section, we will first use a simple drawing interface to draw lines or surfaces in the images of every class. We damage edges as seriously as possible and then produce these damaged images which are shown in Fig. 4-1. Based on these same damaged images from classes a to f, we will compare the proposed method with pure fast digital image inpainting [2] and pure priority texture synthesis [7]. Based on these images from classes g to i, we will use the proposed method to remove some objects. The proposed method has been implemented on PC with Pentium4 1.8G, RAM 1024 Megabytes. The operating system is Microsoft Windows XP Server Chinese version Service Pack2. The program was developed in the C++ language and compiled under Borland C++ Builder version 6.0.

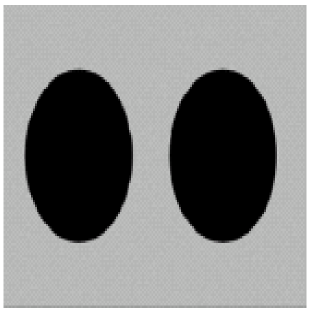
Original image

Original image

Original image

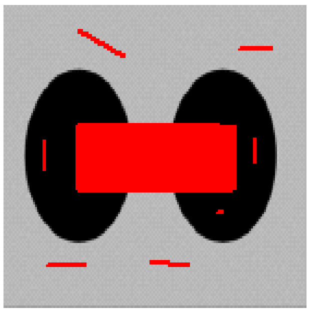
Damaged image

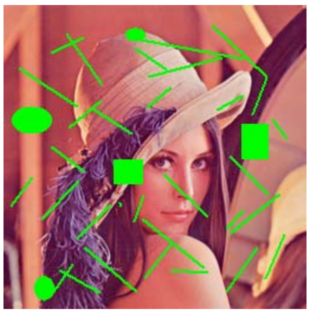
Damaged image

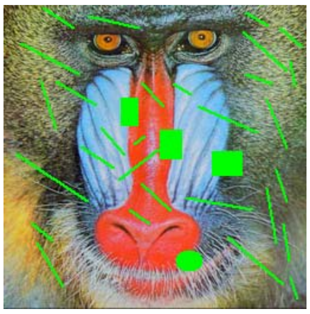
Damaged image

Class a. Elliptic image

Class b. "Lena" image

Class c. "Baboon" image

Original image

Original image

Original image

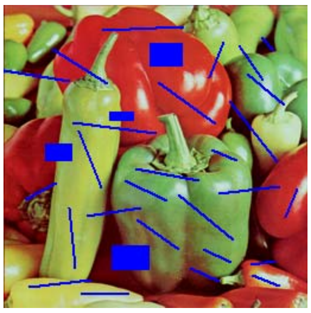
Damaged image

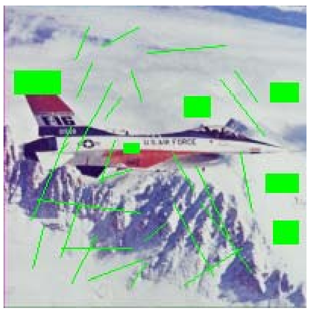
Damaged image

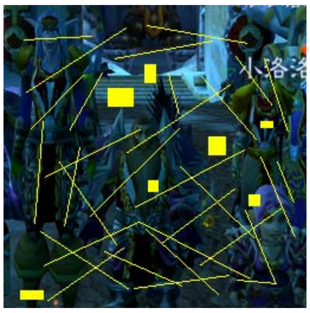
Damaged image

Class d. "Pepper" image

Class e. "F16" image

Class f. Game image

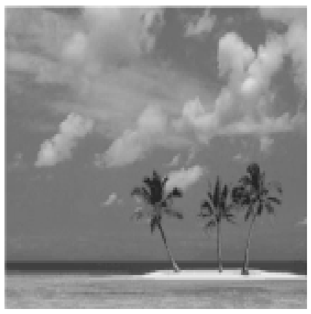

Original image

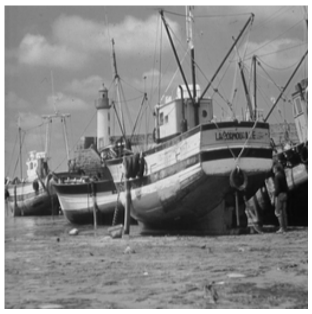

Original image

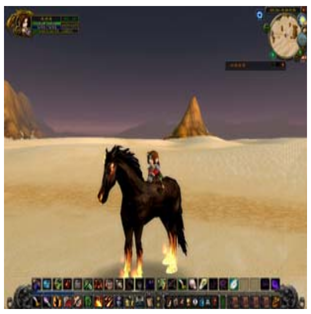

Original image

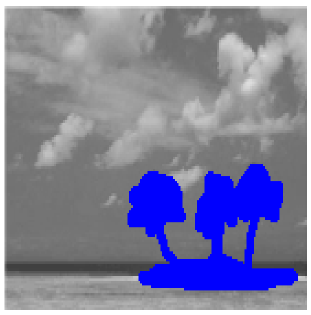

Damaged image

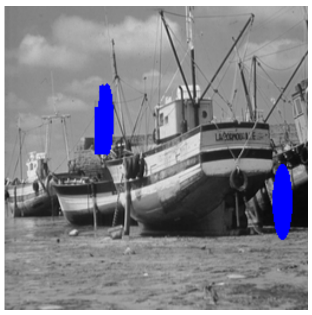

Damaged image

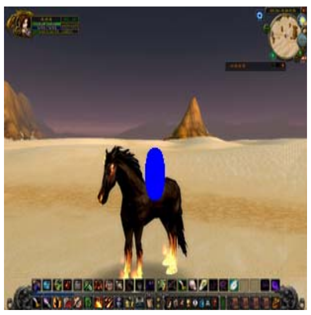

Damaged image

Class g. Tree image **Class h. Fishing Boat image** **Class i. Girl image**

Fig. 4- 1 There are some test images. Top images of every class are original images. Bottom images of every class are damaged images.

4.2 Experimental Results

4.2.1 Comparison of inpainting results

Here, we apply the proposed method to a variety of images. Where possible, we make side-by-side comparisons to two other methods from Fig. 4-2 to 4-11.

Fig. 4-2 (a) is the result of Fast Digital Image Inpainting. It spends 0.032 seconds on inpainting. The central damaged rectangle can’t be inpainted well. Elliptic Edges are blurred; Fig. 4-2 (b) shows its intermediate inpainting steps. (Top-left represents 0% inpainting result. It also means the original damaged image. Top-center and Top-right individually represent 20% and 40 % inpainting result. Bottom-left, Bottom-center and Bottom-right individually represent 60%, 80% and 100 % inpainting result.). Fig. 4-3 (a) is the result of Priority Texture Synthesis. It spends 10.172 seconds on inpainting. The central damaged rectangle can be inpainted well. In order to preserve edge sharpness, this method gives the higher inpainting priority to the edges of damaged parts and starts to inpaint according to their priorities. Fig. 4-4 (a) splits damaged regions into two parts by using “opening” (“Green” represents small damaged parts and “Blue” represents large damaged parts); Fig. 4-4 (b) is the result of the proposed method. It spends 7.454 seconds on inpainting. The central damaged rectangle can be inpainted well. The proposed method inpaint these large damaged parts after inpainting these small damaged parts.

Fig. 4-5 (a) is the result of Fast Digital Image Inpainting. It spends 0.062 seconds on inpainting. The left pillars are blurred. Fig. 4-6 (a) is the result of Priority Texture Synthesis. It spends 52.703 seconds on inpainting. This method preserves edge sharpness. Fig. 4-7 (a) splits damaged regions into two parts by using “opening” (“Red” represents small damaged regions and “Blue” represents large damaged regions); Fig. 4-7 (b) is the result of the proposed method. It spends 20.453 seconds on inpainting. This method not only preserves edge sharpness but also speedups the time. Fig. 4-8 to 4-11 are other examples of inpainting.

At last, we show the proposed method to remove large objects from images. The trees have been completely removed and the occluded region reconstructed by the proposed method in Fig. 4-12. The lighthouse and the fisherman have been completely removed and the occluded region reconstructed by the proposed method in Fig. 4-13. Fig. 4-14 shows some objects which are gradually removed by the proposed method. Finally, the girl on the horse is also removed. Background texture and structure have seamlessly replaced the original characters. Fig. 4-15 shows a personal example of removing an object that can represent me on a highly textured background. (a) I lift up my cousin. (b) I have been removed and my cousin floats in the air. Notice the area of my cousin’s left armpit, it’s expectable to inpaint with flowers and plants because there is no air information.

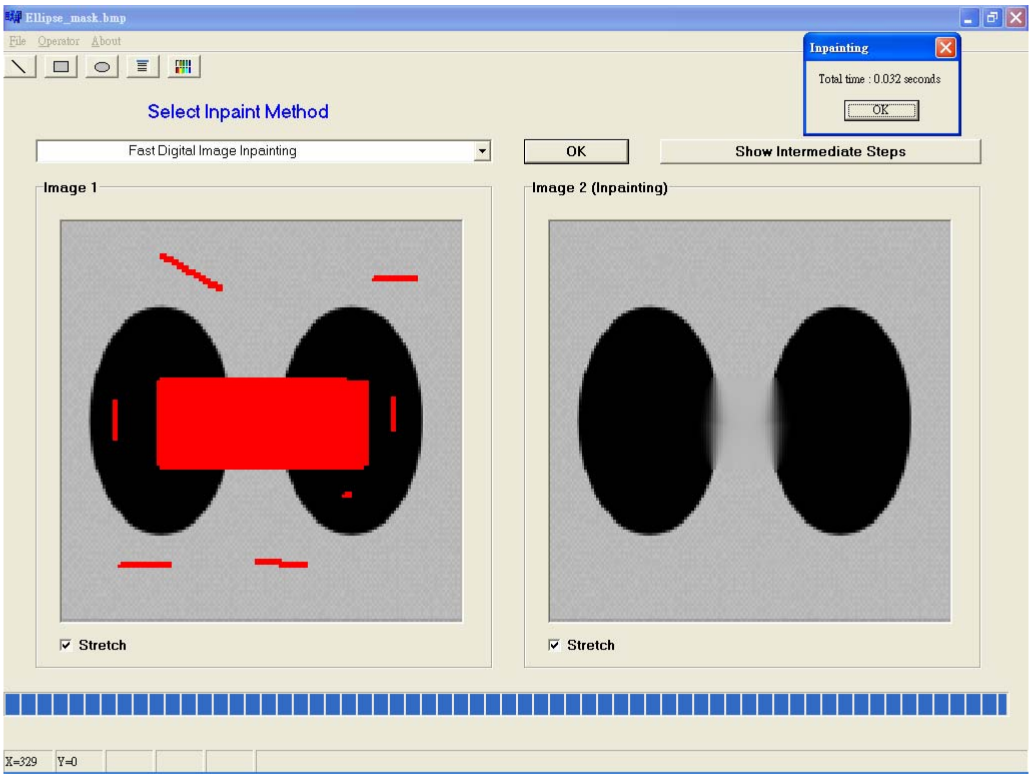

(a)

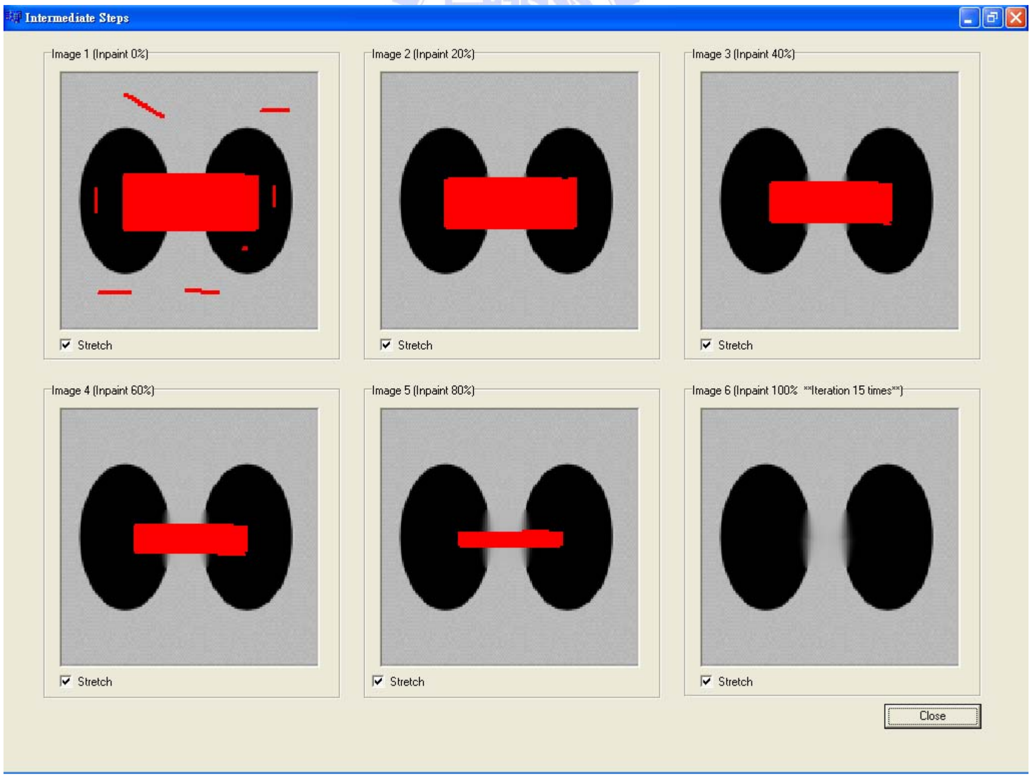

(b)

Fig. 4- 2 (a) The result of Fast Digital Image Inpainting; (b) The intermediate inpainting steps.

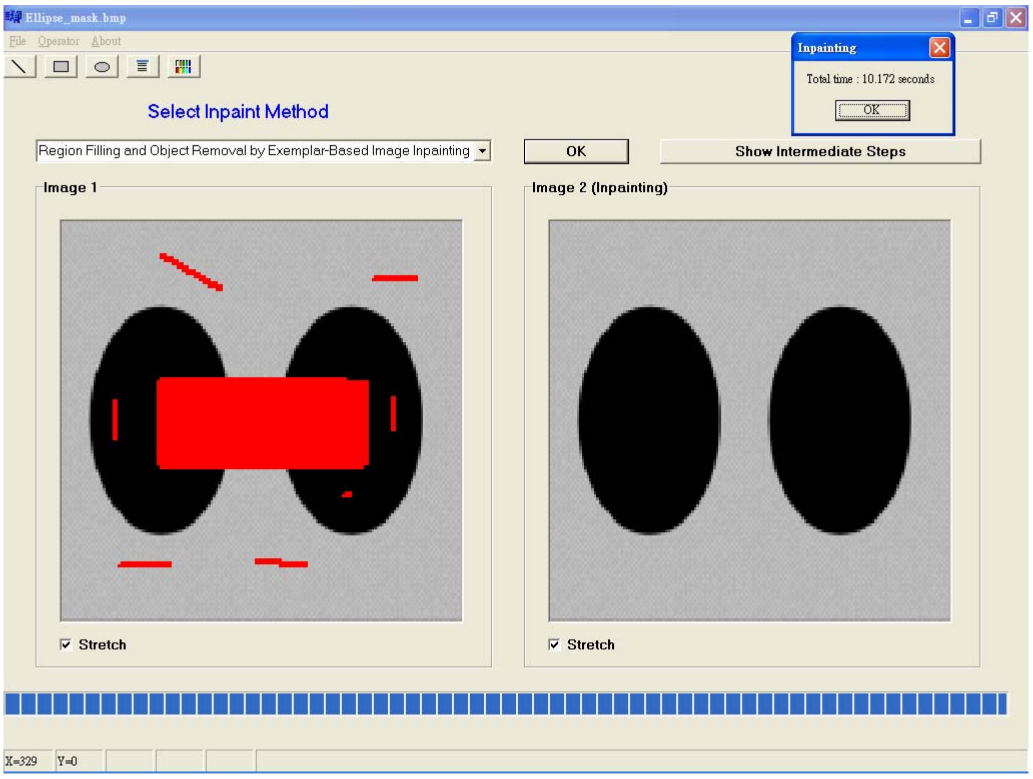

Total time : 10.172 seconds

Region Filling and Object Removal by Exemplar-Based Image Inpainting

(a)

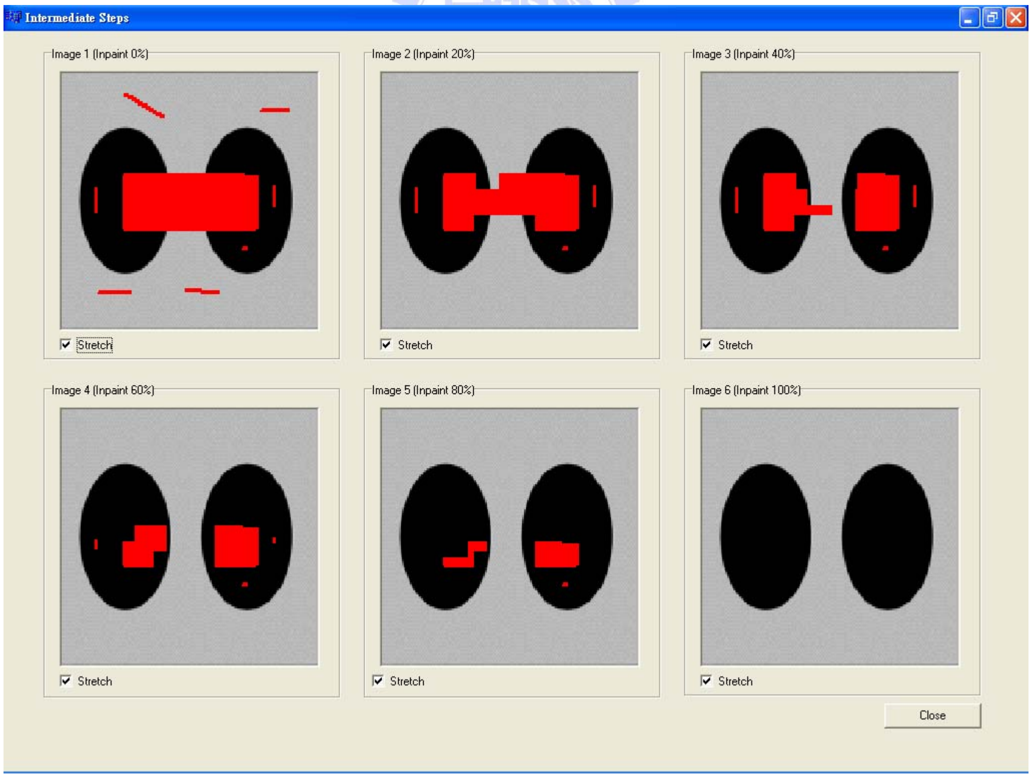

(b)

Fig. 4- 3 (a) The result of Priority Texture Synthesis; (b) The intermediate inpainting steps.

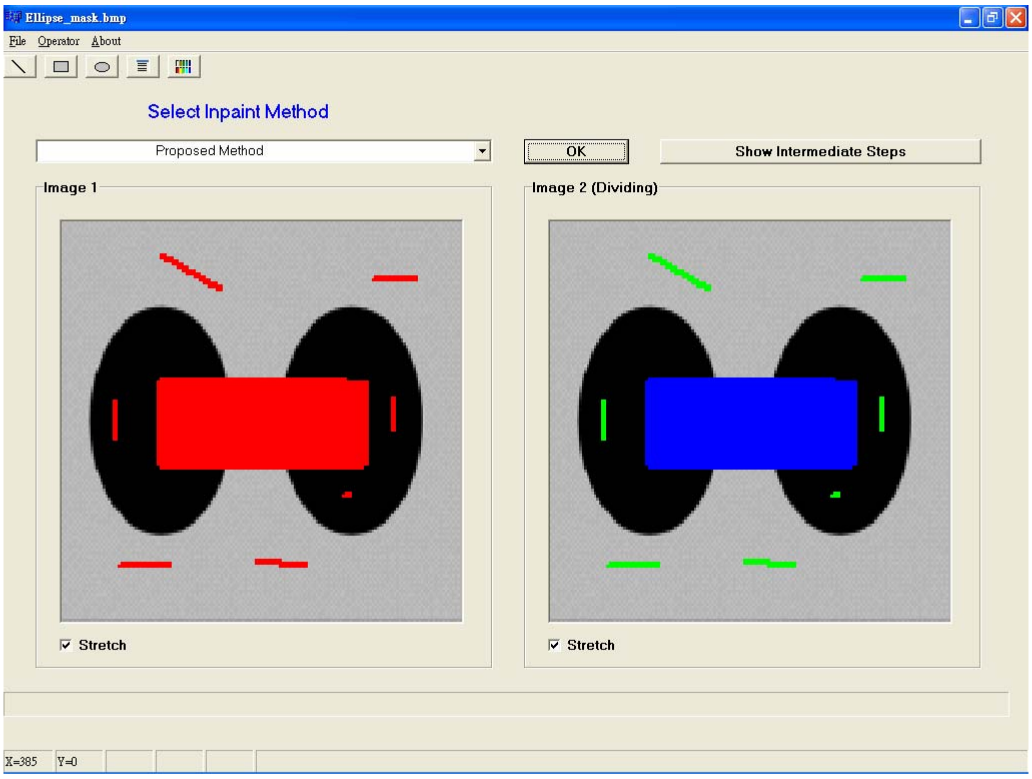

(a)

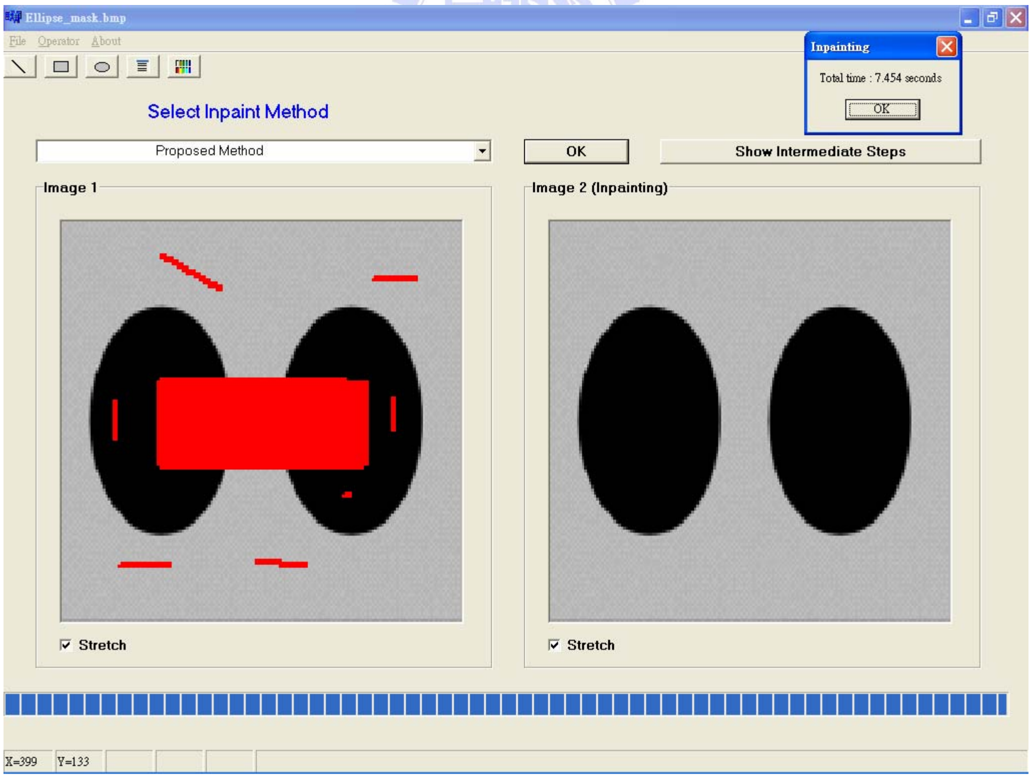

Total time : 7.454 seconds

(b)

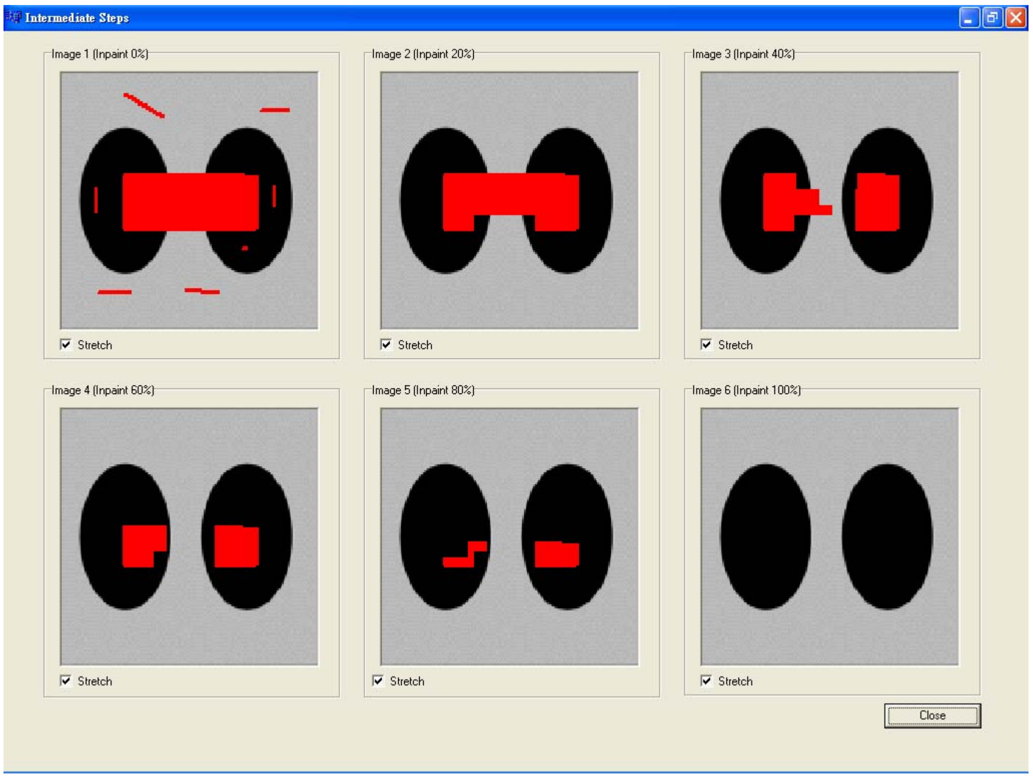

(c)

Fig. 4- 4 (a) Splitting damaged regions into two parts by using "opening"; (b) The result of the proposed method. (c) The intermediate inpainting steps.

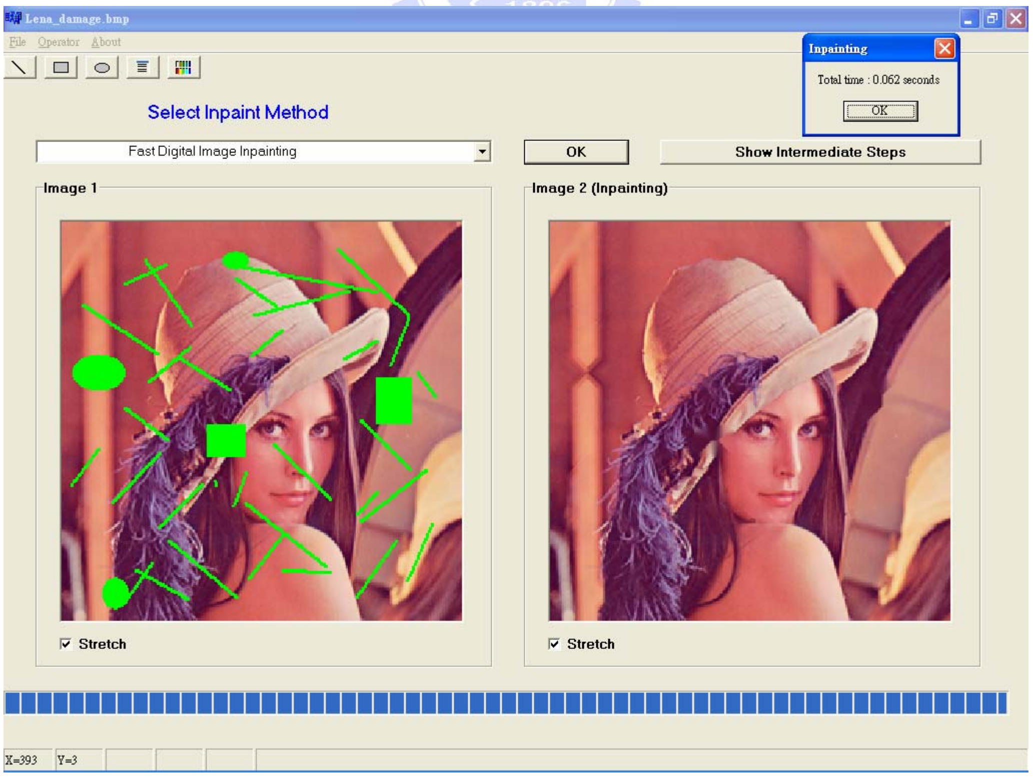

Total time : 0.062 seconds

(a)

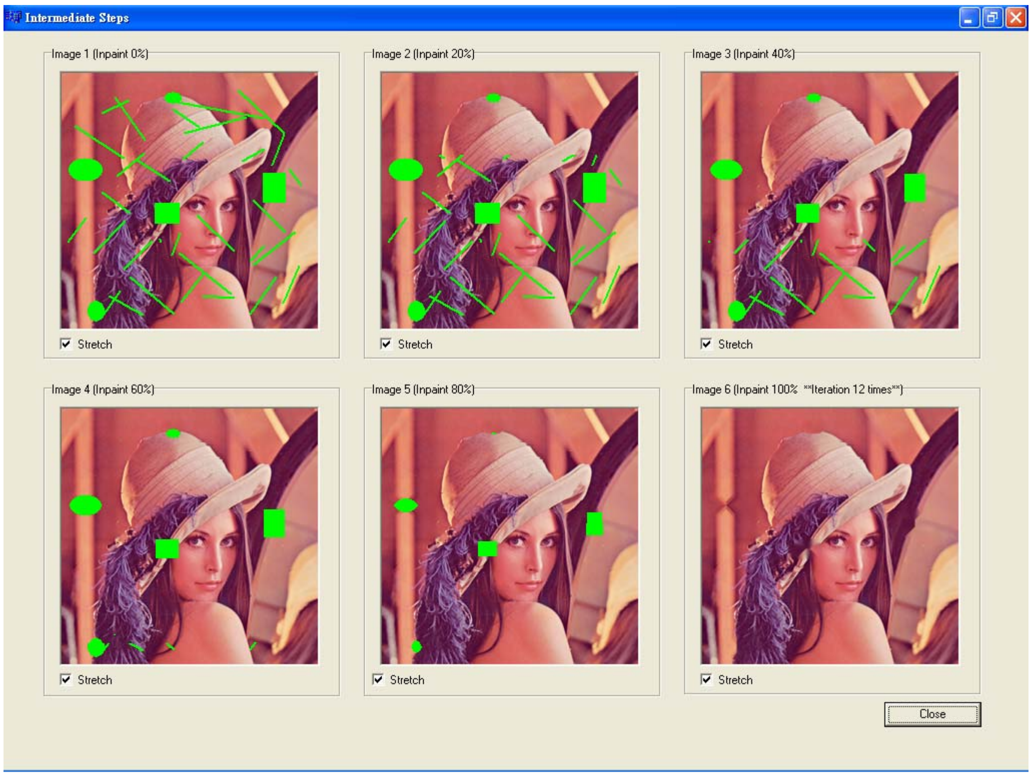

(b)

Fig. 4- 5 (a) The result of Fast Digital Image Inpainting. (b) The intermediate inpainting steps.

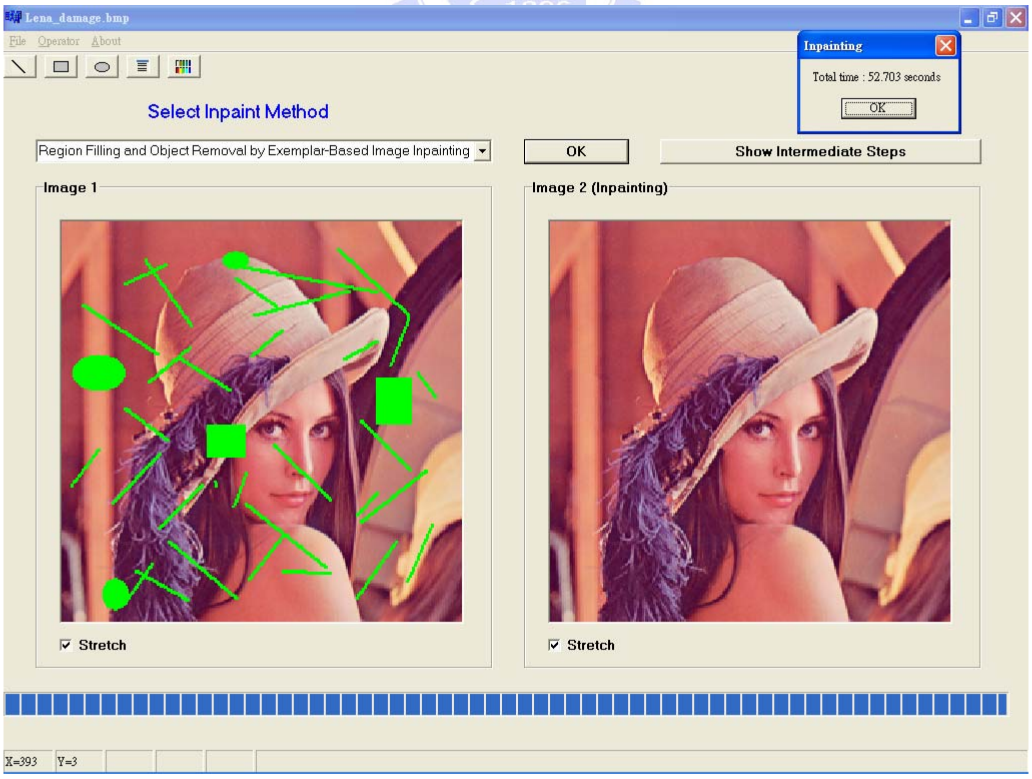

Total time : 52.703 seconds

(a)

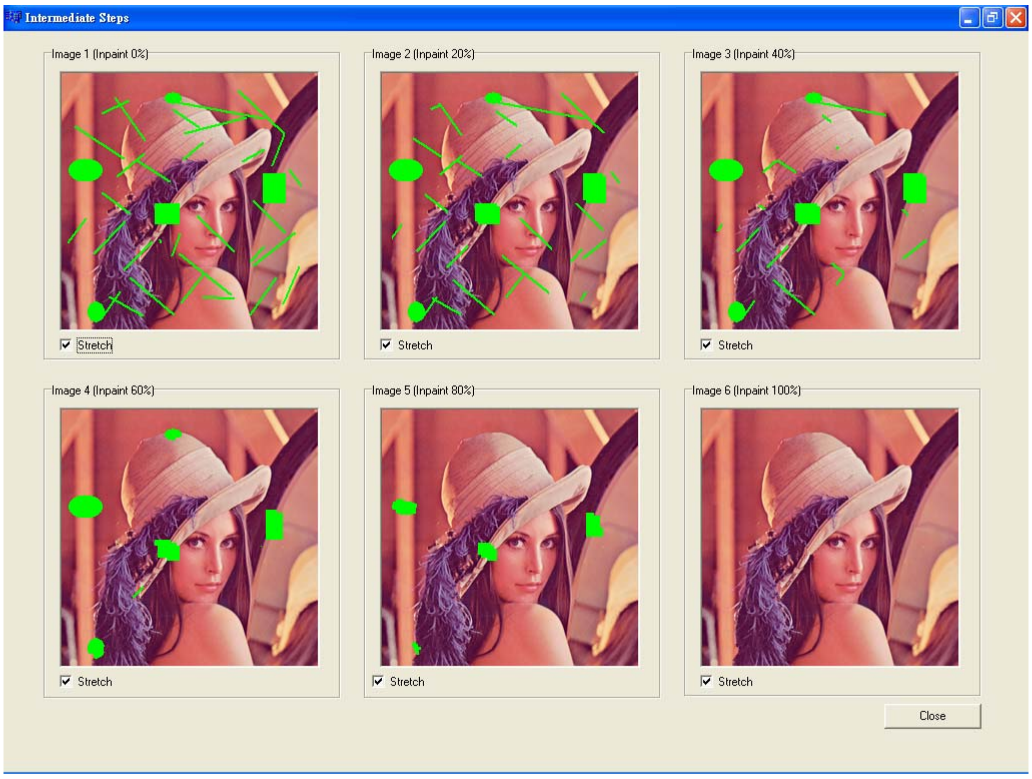

(b)

Fig. 4- 6 (a) The result of Priority Texture Synthesis. (b) The intermediate inpainting steps.

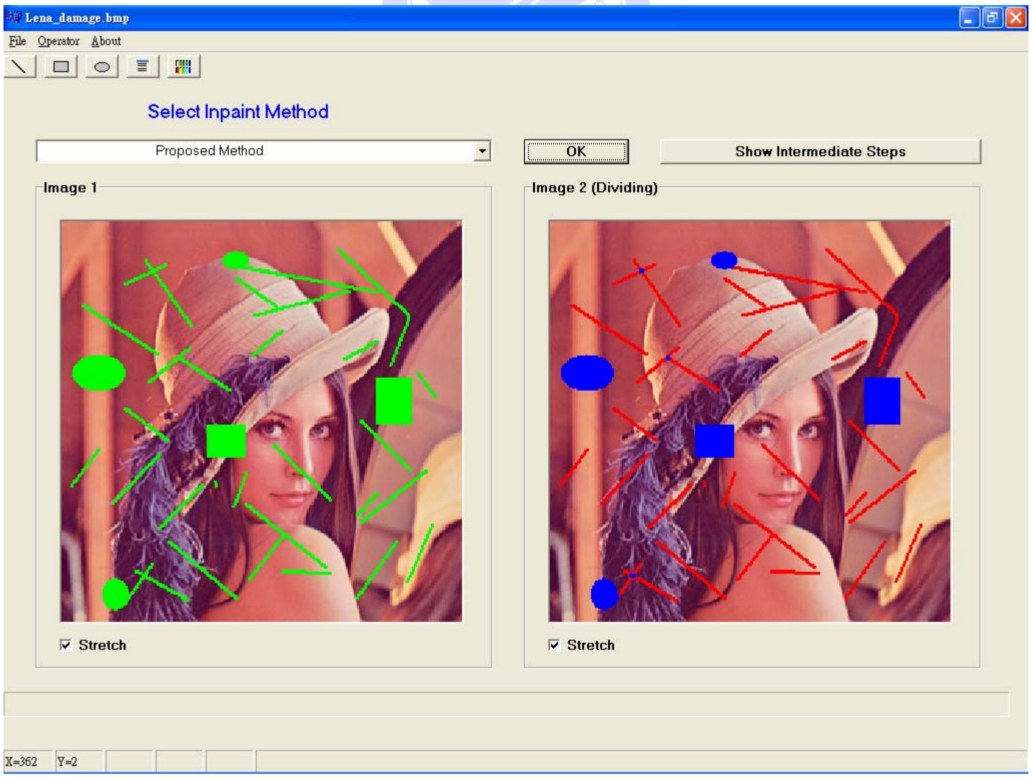

(a)

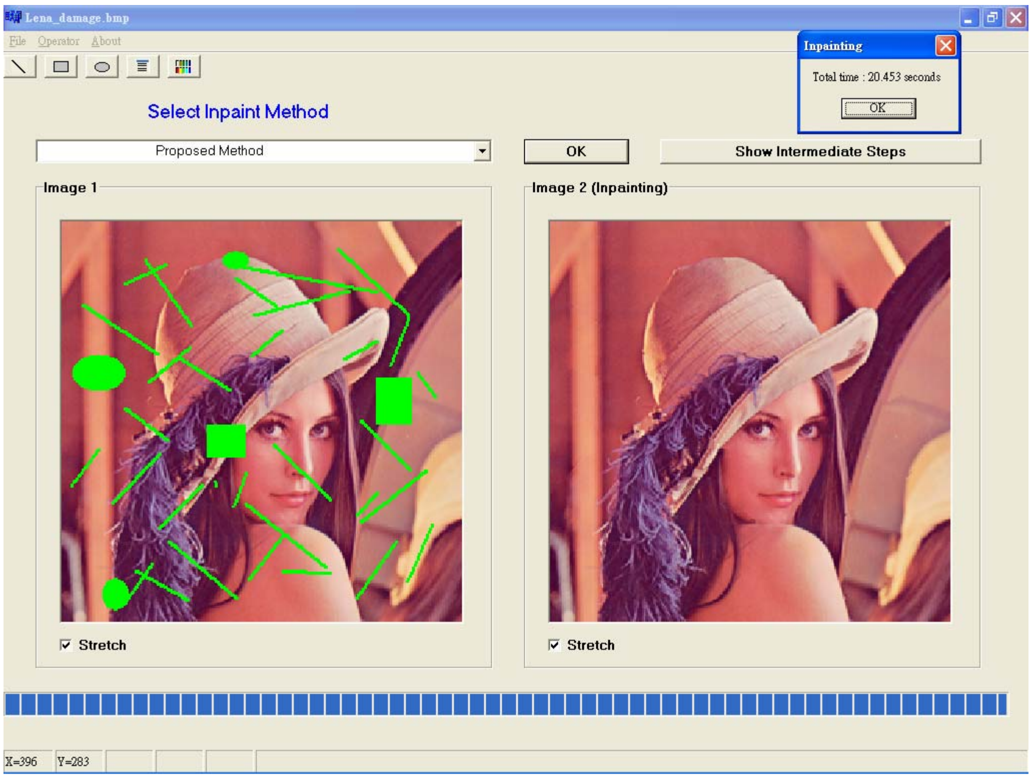

(b)

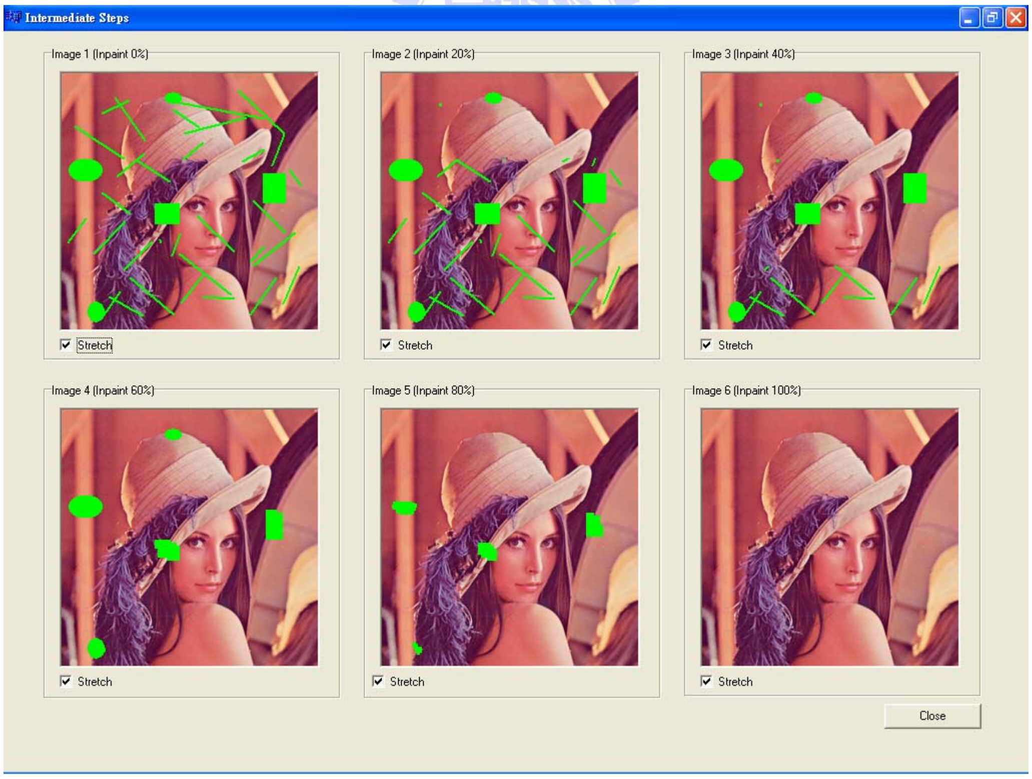

(c)

Fig. 4- 7 (a) Splitting damaged regions into two parts by using "opening"; (b) The result of the proposed method. (c) The intermediate inpainting steps.

(a)

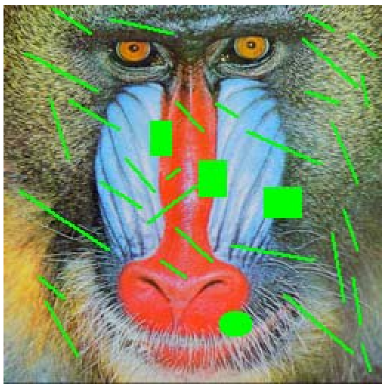
(b)

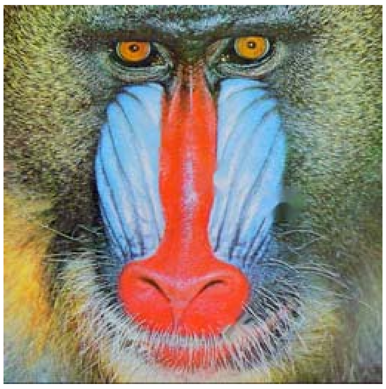
(c)

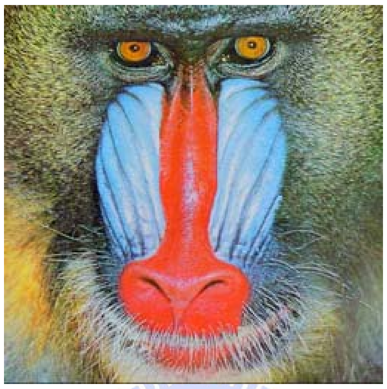
(d)

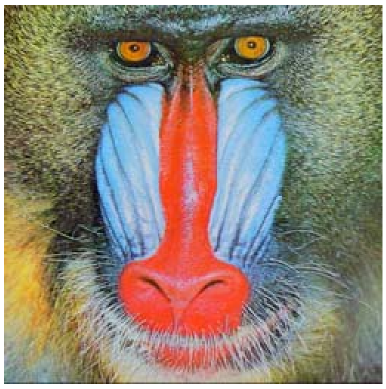
(e)

Fig. 4- 8 (a) Original image (b) Damaged image (c) The inpainting result of Fast Digital Image Inpainting; (d) The inpainting result of Priority Texture Synthesis; (e) The inpainting result of the proposed method. Notice the difference in the nose and face of the baboon between (a), (c), (d) and (e).

(a)

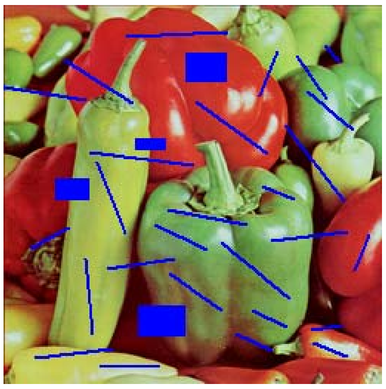
(b)

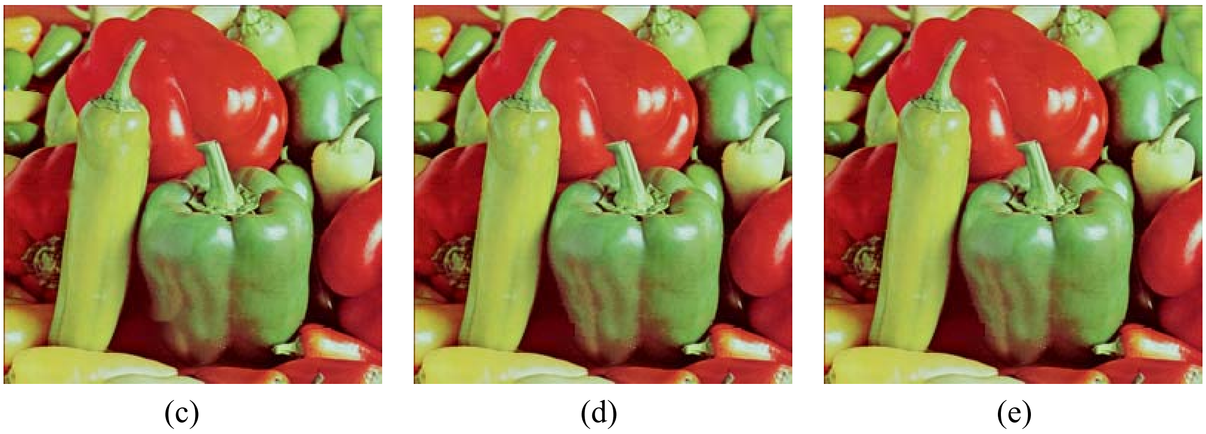

Fig. 4- 9 (a) Original image (b) Damaged image (c) The inpainting result of Fast Digital Image Inpainting; (d) The inpainting result of Priority Texture Synthesis; (e) The inpainting result of the proposed method. Notice the difference in the edges of the pepper between (a), (c), (d) and (e).

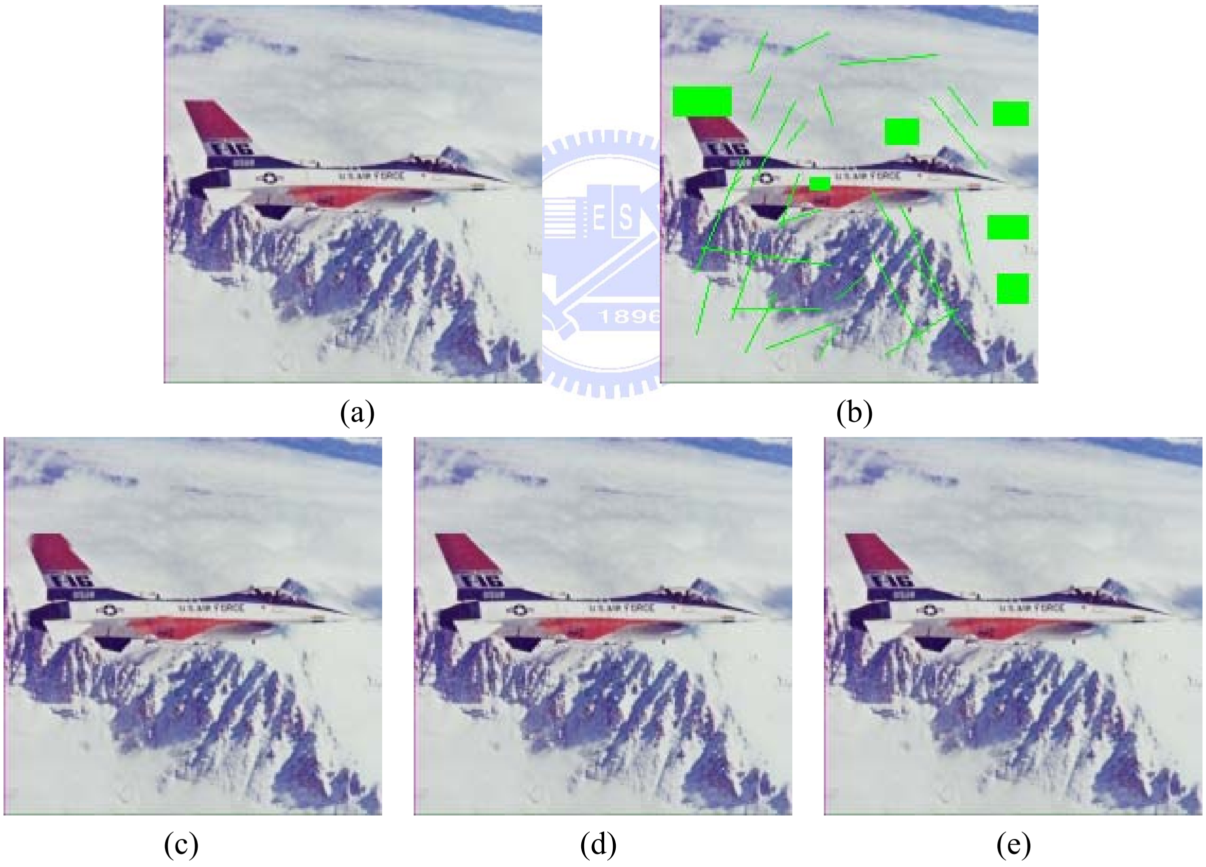

Fig. 4- 10(a) Original image (b) Damaged image (c) The inpainting result of Fast Digital Image Inpainting; (d) The inpainting result of Priority Texture Synthesis; (e) The inpainting result of the proposed method. Notice the difference in the tail wing of the F16 between (a), (c), (d) and (e).

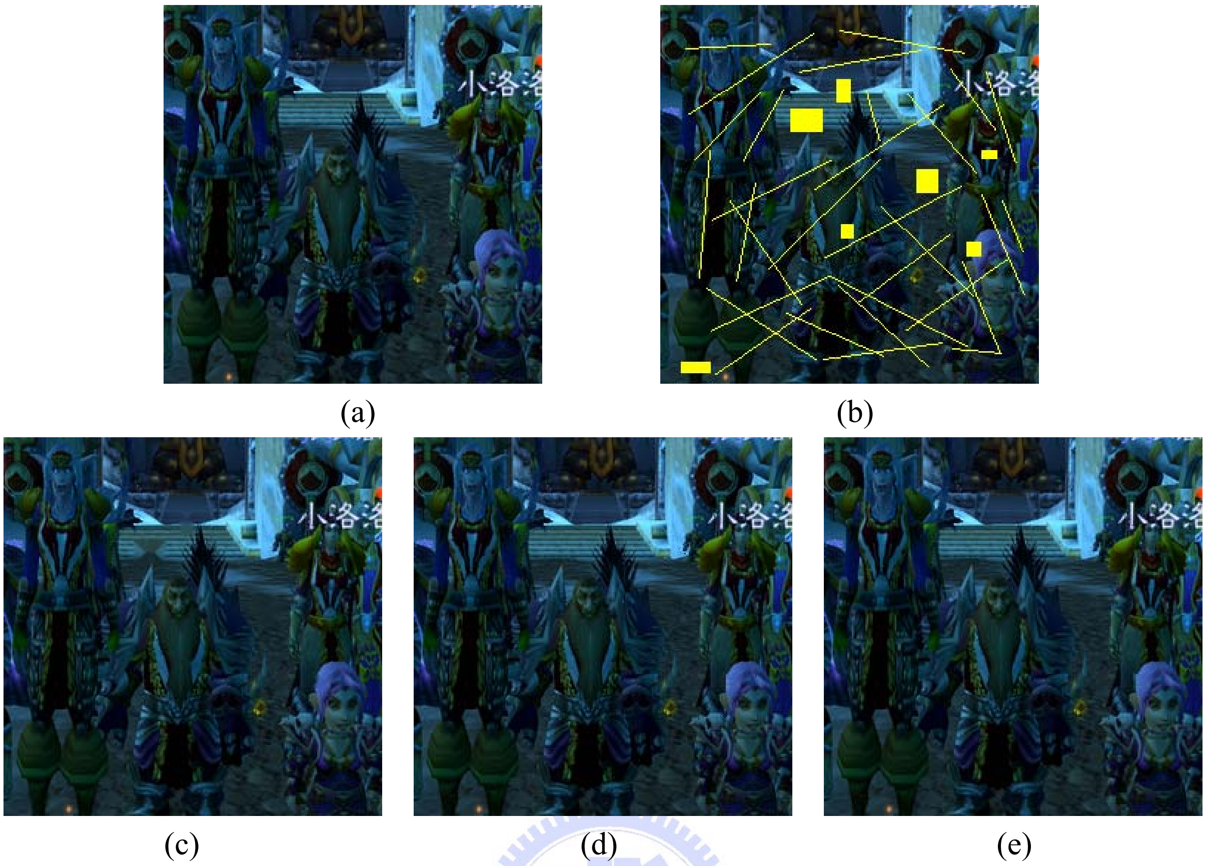

Fig. 4- 11 (a) Original image (b) Damaged image (c) The inpainting result of Fast Digital Image Inpainting; (d) The inpainting result of Priority Texture Synthesis; (e) The inpainting result of the proposed method. Notice the difference in the stairway of the game’s image between (a), (c), (d) and (e).

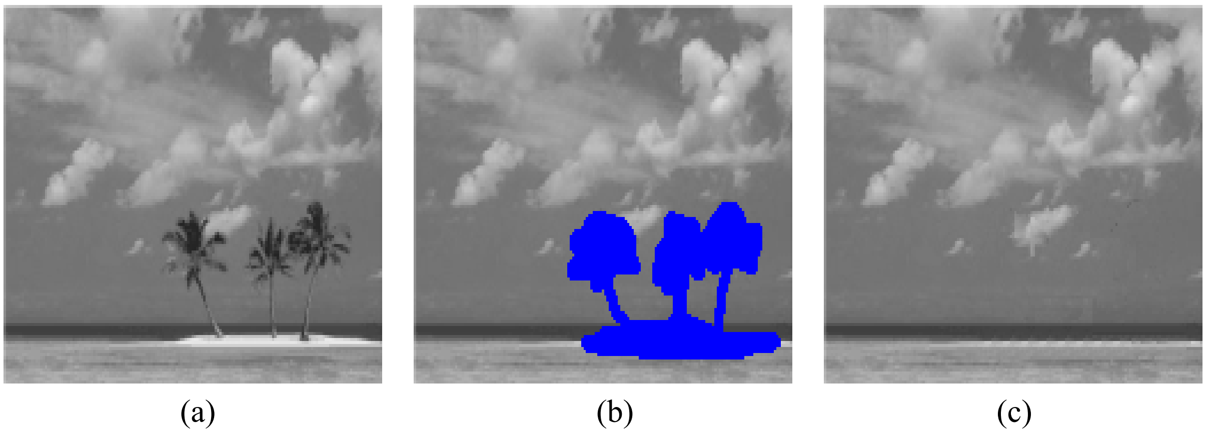

Fig. 4- 12 Removing large objects from images. (a) Original image (b) Mark large objects which we want to remove (c) The removal of trees.

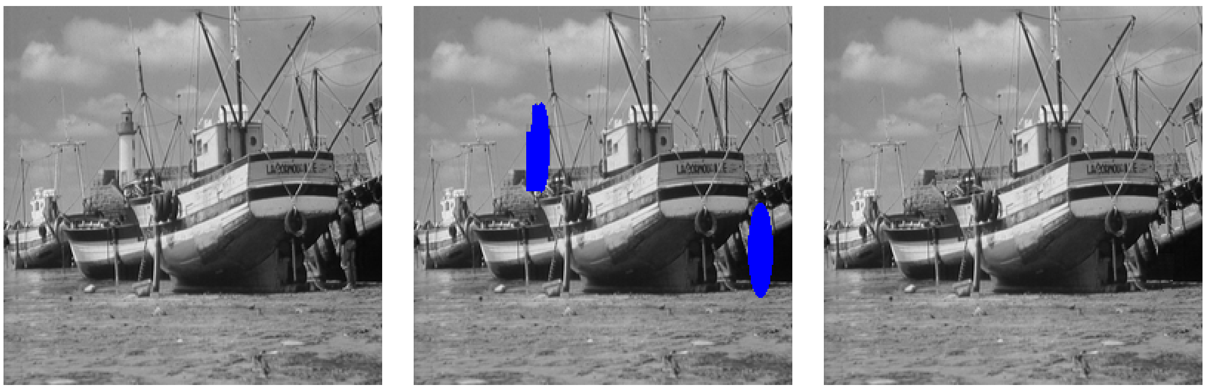
(a) (b) (c)

Fig. 4- 13 Removing large objects from images. (a) Original image (b) Mark large objects which we want to remove (c) The removal of the lighthouse and fisherman.

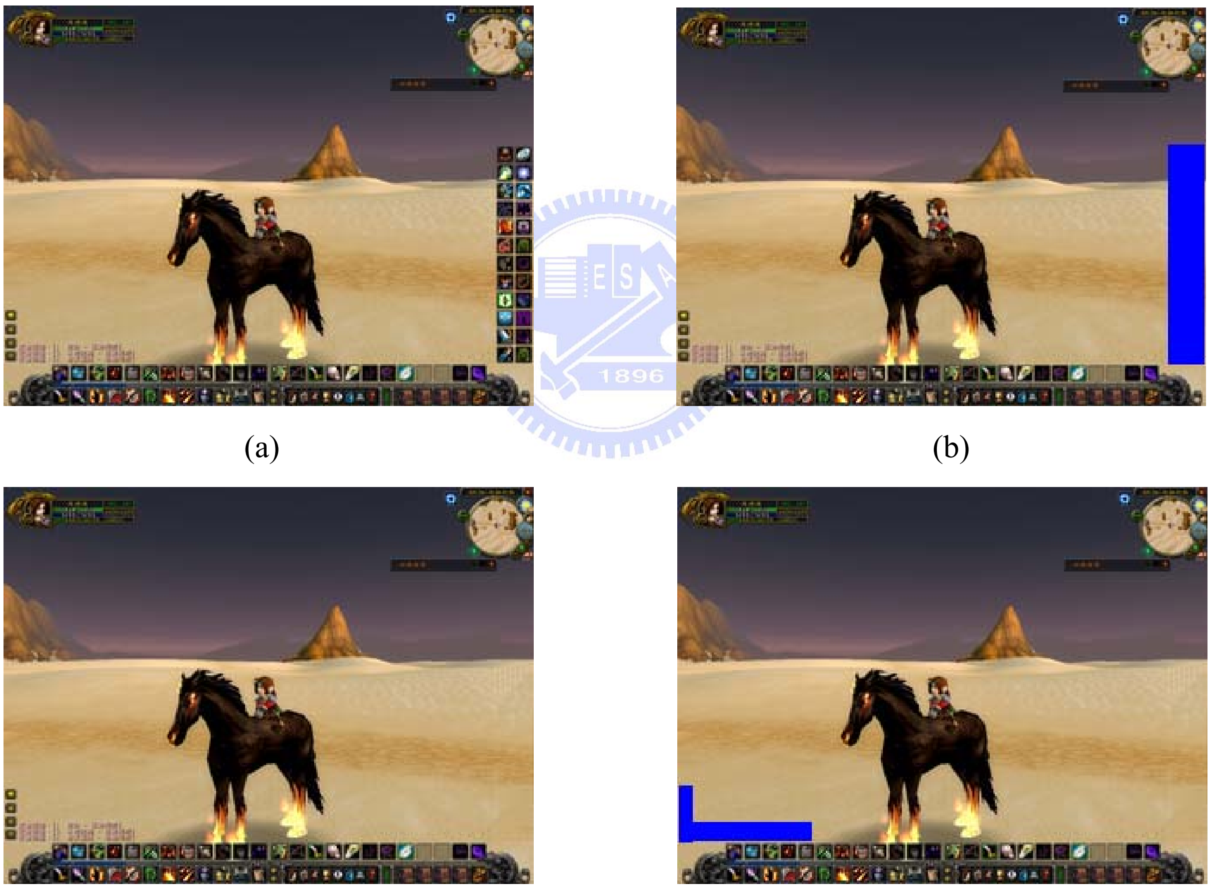
(a) (b)

(c) (d)

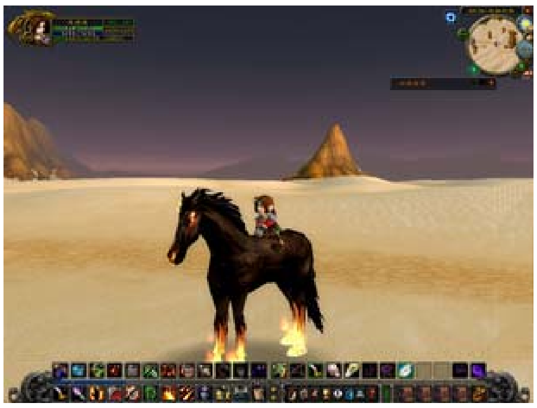

(e)

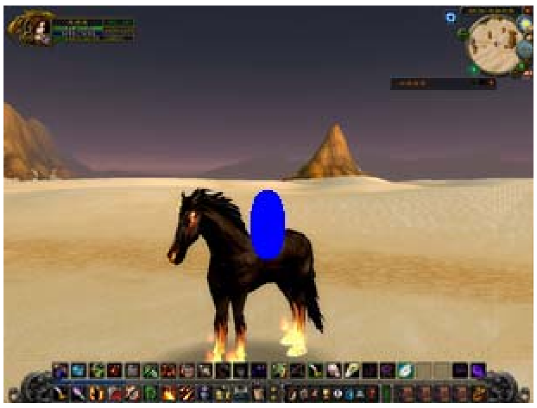

(f)

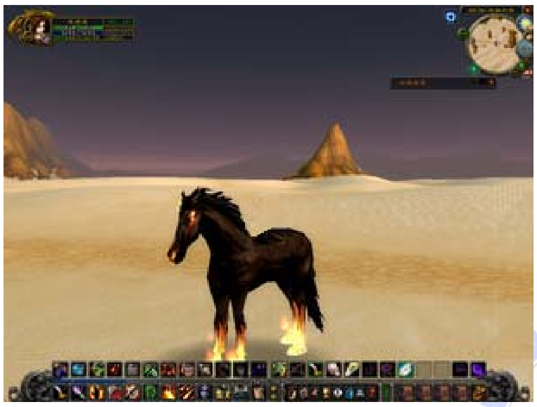

(g)

Fig. 4- 14 Removing several objects from images.

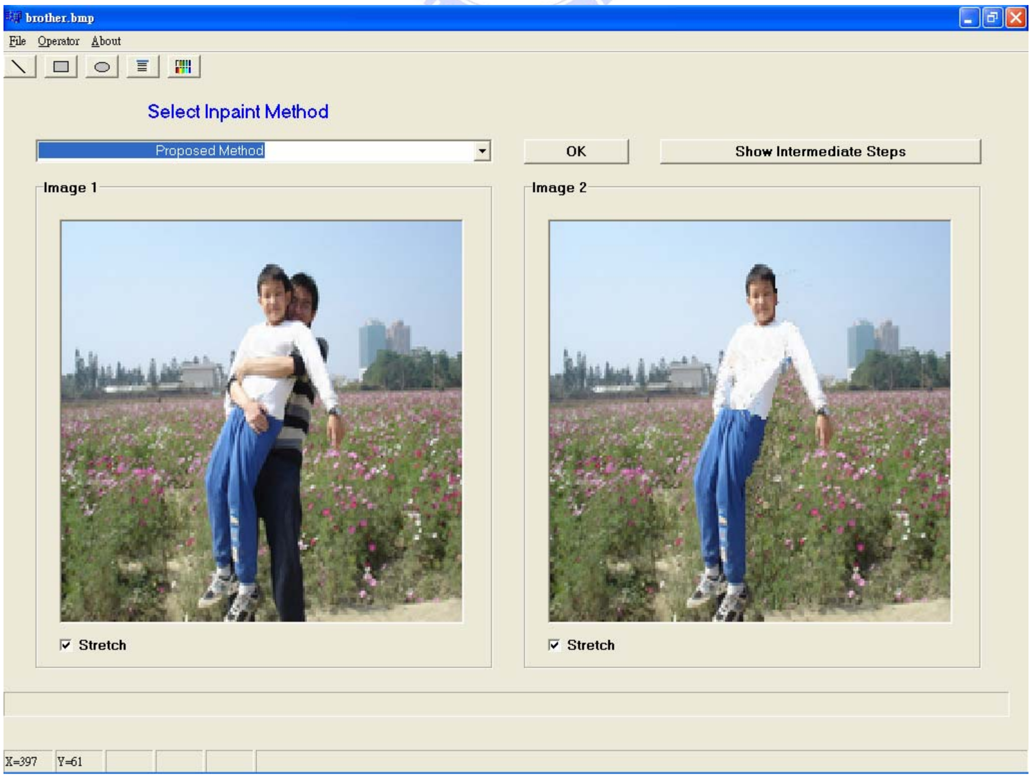

Select Inpaint Method

Proposed Method

X=397 Y=61

Fig. 4- 15 Special effects (my cousin and me)

4.2.2 Comparison of PSNR Values

In a practical situation, it is impossible to compare a damaged picture with its original. However, the strategy of our evaluation is based on the following assumption. Suppose that there are two copies of the original picture. The second is damaged, and we will like to recover the damage as much as possible such that the inpainted image will look almost the same as the first original. Then, we can compute a PSNR value that reflects the quality of a inpainted image. As seen in Table 4-1, The PSNR values of the proposed method and Pure Priority Texture Synthesis are almost higher than Pure Fast Image Inpainting. It may indicate that the proposed method and Pure Priority Texture Synthesis can inpaint the damaged images better than Pure Fast Image Inpainting. Notice that the PSNR value isn't suited to compare these images obtained from some large objects which users want to remove. (such as Fig. 4-12 to 4-15).

Methods / Test Images	Pure Fast Image Inpainting	Pure Priority Texture Synthesis	Proposed Method
Elliptic Image	29.100	42.768	42.700
Lena	32.351	35.818	36.238
Baboon	30.178	31.603	32.716
Pepper	37.784	38.315	38.338
F16	36.089	38.950	40.344
Game’s image	38.178	38.225	40.644

Table 4- 1 Comparison of PSNR Values

4.2.3 Comparison of Running Time

Table 4-2 shows the total inpainting time. Viewing from the analysis, Pure Fast Image Inpainting is faster than two other methods, but it can’t inpaint well for large damaged regions. The proposed method and Pure Priority Texture Synthesis can both inpaint well for large damaged regions, and the proposed method is faster than Pure Priority Texture Synthesis in the same situation (+FFT). If there are more small damaged regions in the images, the proposed method is more faster than Pure Priority Texture Synthesis.

Methods / Test Images	Pure Fast Image Inpainting	Pure Priority Texture Synthesis (+FFT)	Proposed Method (+FFT)
Elliptic Image Size:164*126 Damaged regions: 13.318%	0.032	10.172	7.454
Lena Size:256*256 Damaged regions: 7.53%	0.062	52.703	20.453
Baboon Size:256*256 Damaged regions: 6.064%	0.063	64.891	19.812
Pepper Size:256*256 Damaged regions: 6.433%	0.061	64.656	19.151
F16 Size:200*200 Damaged regions: 6.325%	0.046	22.672	8.532
Game's image Size:256*256 Damaged regions: 4.929%	0.059	62.016	9.719

Table 4- 2 Comparison of Running Time

CHAPTER 5
Conclusions and Future Works

5.1 Conclusions

In this study, we propose an image inpainting method that will combine "Fast Digital Image Inpainting" and "Priority Texture Synthesis". First, we utilize the morphological operator "opening" to split the damaged regions of images into several small and large parts according to the structuring element which users set up. After splitting, we modify the "Fast Digital Image Inpainting" algorithm and apply it to inpaint these small damaged parts. Then, we use "Priority Texture Synthesis" to inpaint these large damaged parts and add the FFT block matching algorithm to speedup the time of searching similar textures. At last, the system will not only show the inpainted result but also show several intermediate steps of the inpainting on the interface.

From the results shown in Chapter 4, we can conclude that the proposed method has some advantages as described below :

1. Morphologigical operators involve simple logical operations and can be easily implemented. The "opening" operation can efficiently split the damaged regions into several small and large parts.
2. The modification of "Fast Digital Image Inpainting" algorithm can inpaint these locally small damaged parts more efficiently.
3. The proposed method can inpaint large damaged regions well but "Fast Digital Image Inpainting" can't.
4. Although the proposed method and Pure Priority Texture Synthesis can both inpaint large damaged regions well, the proposed method is faster than Pure Priority Texture Synthesis. On average, for images with several small and large damaged regions (Image Size is

256*256 and Damaged Percentage is about 7%), only 18 seconds is needed to inpaint by the proposed method. Pure Priority Texture Synthesis is needed 58 seconds to do the same work in our implement process. If there are more small damaged regions, the proposed method is more faster than Pure Priority Texture Synthesis. It verifies the speed of the proposed method.

5.2 Future works

Future work can be directed to the following topics. First, we would like to put into practice is to add “fuzzy mask” to re-inpaint the damaged image, i.e. a mask where each pixel has a probability between 0.0 and 1.0 instead of a binary true/false. Such masks would be useful to create smooth transitions between the content of the image that is kept and the modified pixels. Second, it is desirable to remove defects or disturbing objects in a fully automatic way.

References

[1] M. Bertalmio, G. Sapiro, V. Caselles and C. Ballester, "Image Inpainting", *ACM SIGGRAPH Conference on Computer Graphics,* pp.417-424, 2000.

[2] Manuel M. Oliveira, Brian Bowen, Richard McKenna, Yu-Sung Chang, "Fast Digital Image Inpainting", *International Conference on Visualization, Imaging and Image Processing (VIIP 2001),* pp. 261-266, 2001.

[3] A. A. Efros and T. K. Leung, “Texture Synthesis by Nonparametric Sampling”, *In IEEE International Conf. on Computer Vision, volume 2*, pp. 1033–1038, 1999.

[4] H. Yamauchi, J. Haber, H.-P. Seidel, “Image Restoration using Multiresolution Texture Synthesis and Image inpainting”, *Computer Graphics International,* pp. 108-113, 2003

[5] S. D. Rane, G. Sapiro and M. Bertalmio, ”Structure and Texture Filling-In of Missing Image Blocks in Wireless Transmission and Compression Applications”, *IEEE Transactions on Image Processing*, vol. 12, no. 3, pp. 296-303, 2003.

[6] A. Criminisi, P. Pérez and K. Toyama, “Object Removal by Exemplar-Based Inpainting”, *in Proc. Conf. Computer Vision and Pattern Recognition*, Madison, WI, 2003.

[7] A. Criminisi, P. Pérez and K. Toyama, “Region Filling and Object Removal by Exemplar-Based Image Inpainting” (“Priority Texture Synthesis”), *IEEE Transactions on Image Processing*, vol. 13, no. 9, pp. 1200-1212, 2004.

[8] M. Bertalmio, L. Vese, G. Sapiro, and S. Osher, “Simultaneous Structure and Texture Image Inpainting”, *in Proc. Conf. Comp. Vision Pattern Rec.*,Madison, WI, pp. 882-889, 2003.

[9] R. Bornard, E. Lecan, L. Laborelli and J.-H. Chenot, “Missing Data Correction in Still Images and Image Sequences,” *in ACM Multimedia,* France, pp. 355-361, 2002.

[10] Steven L. Kilthau, Mark S. Drew, and Torsten Möller, “Full Search Content Independent Block Matching Baded On The Fast Fourier Transform,” *IEEE ICIP*, pp. 669-672, 2002.

[11] Timothy K. Shih, Rong-Chi Chang and Liang-Chen Lu, “Adaptive Digital Image Inpainting”, *in proceedings of the 18th International Conference on Advanced Information Networking and Applications (AINA 2004)*, Japan, March 29 - 31, 2004.

[12] J. S. D. Bonet, “Multiresolution Sampling Procedure for Analysis and Synthesis of Texture Images”, *In SIGGRAPH ’97*, pp. 361–368, 1997.

[13] T. F. Chan and J. Shen, “Non-Texture Inpainting by Curvature-Driven Diffusions (CDD)”, *J. Vis. Comm. Image Rep.*, vol. 4, no. 12, pp. 436–449, 2001.

[14] C. Ballester, V. Caselles, J. Verdera, M. Bertalmio, and G. Sapiro, “A Variational Model for Filling-in Gray Level and Color Images”, *In Proc. ICCV,* pp. I: 10–16, Vancouver, Canada, 2001.

[15] M. Beltalmio, A. Bertozzi, G. Sapiro, “Navier-Stokes, Fluid-Dynamics and Image and Video Inpainting”, *in Proceedings of the 2001 IEEE Computer Society Conference on Computer Vision and Pattern Recognition*, pp. 1355-1362, 2001.

[16] D. Garber, “Computational Models for Texture Analysis and Texture Synthesis”, Ph.D. dissertation, Univ. Southern California, Los Angeles, CA, 1981.

[17] C:H. Huang; J.-L. Wu, “Inpainting Attacks against Visible Watermarking Schemes”, *in Proceedings of Spie, the International Society for Optical Engineering*, no. 4314, pp. 376-384, 2001.

[18] A. A. Efros and W. Freeman, “Image Quilting for Texture Synthesis and Transfer”, presented at the *Proc. SIGGRAPH*, 2001.

[19] L.-W. Wey and M. Levoy, “Fast Texture Synthesis Using Tree-Structured Vector Quantization,” *in Proc. ACM Conf. Computer Graphics (SIGGRAPH)*, 2000.

[20] G. Gorla, V. Interrante, and G. Sapiro, “Growing Fitted Textures,” *IEEE Trans. Visual. Comput. Graphics*, to be published.

[21] Gomes, J., Velho, L. *Image processing for computer graphics* (New York, NY, Springer-Verlag, 1997)

[22] S. Osher and J. Sethian, “Fronts Propagating with Curvature Dependent Speed: Algorithms Based on Hamilton-Jacobi Formulations”. *Journal of Computational Physics*, 79, pp.12-49, 1988.

[23] Shuntaro YUI, Kenji HARA, Hongbin ZHA, adn Tsutomu HASEGAWA, “A Fast Narrow Band Method and Its Application in Topology-Adaptive 3-D Modeling”, *IEEE*, pp. 122-125, 2002.

[24] F. C. Crow, “Summed-Area Tables for Texture Mapping,” *Computer Graphics (Proc. of Siggraph)*, pp. 207-212, 1984.

[25] R. C. Gonzalez and R. E. Woods, “Digital Image Processing,” Addision Wesley, Reading, Massachusetts, 1992.

[26] C. R. Giardina and E. R. Dougherty, “Morphological Methods in Image and Signal Processing,” Prentice Hall, New Jersey, 1988.

[27] A. C. Kokaram, R. D. Morris, W. J. Fitzgerald, and P. J. W. Rayner, “Detection of Missing Data in Image Sequences.” *IEEE Trans. Image Processing*, vol. 4, no. 11, pp. 1496–1508, Nov. 1995.